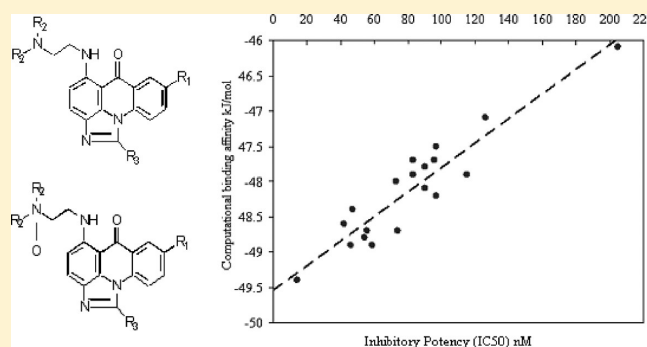


Novel Inhibitors of NRH:Quinone Oxidoreductase 2 (NQO2):
Crystal Structures, Biochemical Activity, and Intracellular Effects
of Imidazoacridin-6-ones[†]Mark S. Dunstan,[‡] John Barnes,^{§,||} Matthew Humphries,[§] Roger C. Whitehead,^{||} Richard A. Bryce,[§]
David Leys,[‡] Ian J. Stratford,[§] and Karen A. Nolan^{*,§}[‡]Manchester Interdisciplinary Biocentre, [§]School of Pharmacy and Pharmaceutical Sciences, and ^{||}School of Chemistry,
University of Manchester and Manchester Cancer Research Centre, Manchester M13 9PT, U.K.

S Supporting Information

ABSTRACT: Imidazoacridin-6-ones are shown to be potent nanomolar inhibitors of the enzyme NQO2. By use of computational molecular modeling, a reliable QSAR was established, relating inhibitory potency with calculated binding affinity. Further, crystal structures of NQO2 containing two of the imidazoacridin-6-ones have been solved. To generate compounds with reduced off-target (DNA binding) effects, an *N*-oxide moiety was introduced into the tertiary aminoalkyl side chain of the imidazoacridin-6-ones. This resulted in substantially less toxicity in a panel of eight cancer cell lines, decreased protein binding, and reduced DNA binding and nuclear accumulation. Finally, one of the *N*-oxides showed potent ability to inhibit the enzymatic function of NQO2 in cells, and therefore, it may be useful as a pharmacological probe to study the properties of the enzyme *in vitro* and *in vivo*.



INTRODUCTION

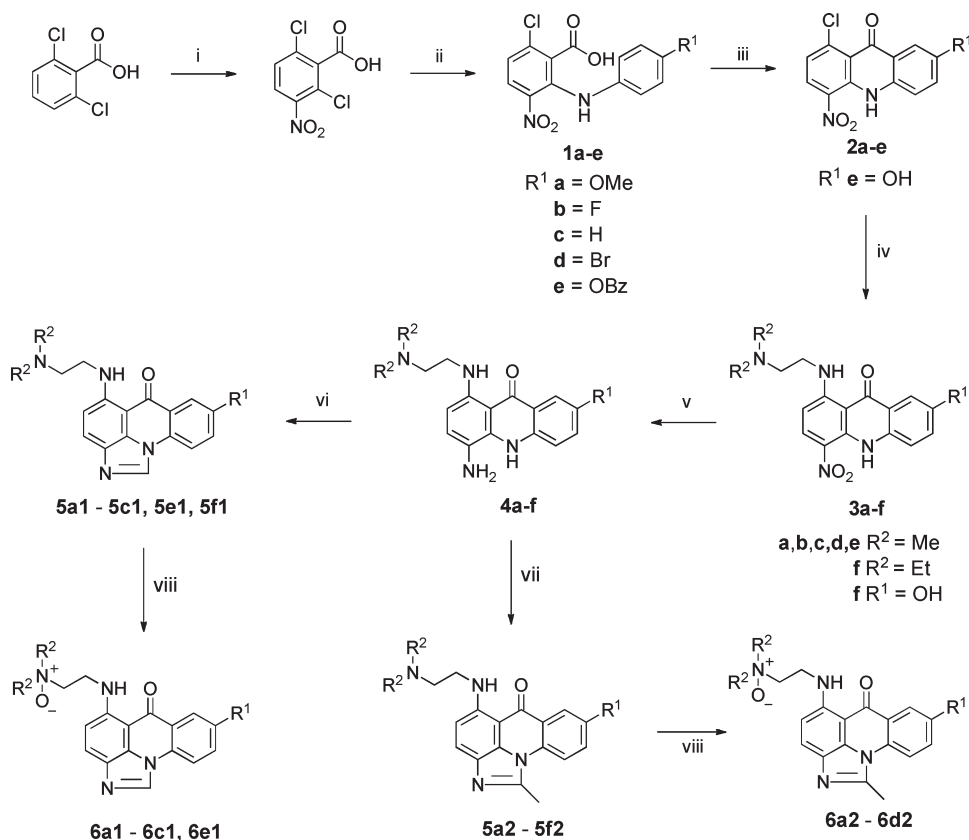
The oxidoreductases NQO1 (NAD(P)H:quinone oxidoreductase 1, QR1, DT-diaphorase, EC 1.6.99.2) and NQO2 (NRH:quinone oxidoreductase 2, QR2, EC 1.10.99.2) are cytosolic flavoproteins that catalyze the oxygen independent, two electron reduction of quinones to hydroquinones.^{1,2} The physiological role of NQO1 is well characterized with its major function being considered to be as a detoxification enzyme.³ A detoxification and/or chemoprotectant role for NQO2 has also been inferred from studies on orthoquinone reduction² and the enhanced carcinogen activity of benzo(a)pyrene observed in NQO2^{-/-} mice.⁴ However, a comparable metabolic role for NQO1 and NQO2 is confounded by the observation that genetic knockout of NQO1 increases menadione toxicity in mice, whereas in NQO2 knockout mice there is protection against menadione toxicity.^{5,6} This has led to the consideration that pharmacological inhibition of NQO2 activity could have some chemoprotectant potential,⁷⁻⁹ a notion supported by the fact that the classical inhibitor of NQO2 is the chemoprotective agent resveratrol.¹⁰ A variety of structurally diverse inhibitors of NQO2 have been identified,^{7-9,11-16} and some of these, imatinib and melatonin, have been shown to protect against radiation induced lung injury.^{17,18} However, these latter agents, as well as resveratrol, have other substantive pharmacological properties, which make them less than ideal for probing the cellular function of NQO2.

We have recently carried out a virtual screening of the National Cancer Institute (NCI) chemical database to identify

potent, novel inhibitors of NQO1 and NQO2.¹¹⁻¹³ From these studies we identified a series of imidazoacridin-6-ones that, from computational molecular modeling, showed excellent predicted binding characteristics to NQO2. Samples of these compounds were supplied by NCI and evaluated for their ability to inhibit human, recombinant NQO2. Inhibitory activity correlated strongly with computational binding affinity, and further, the inhibitory potency of these compounds was the highest yet reported.¹³ Here, we report the synthesis of further imidazoacridin-6-ones in order to confirm our previous findings and provide guidance for the development of potentially pharmacologically active compounds. We have solved the crystal structure of NQO2 containing a parent imidazoacridin-6-one and its *N*-oxide analogue, and this has aided in the preparation of a quantitative structure-activity relationship (QSAR) model. All the compounds inhibit NQO2 at nanomolar concentrations, and their toxicity has been determined in HCT116 colon cancer cells. From the panel of compounds, several were selected for additional biochemical and biological evaluation in order to aid drug development. From a comparison of a parent imidazoacridin-6-one with an *N*-oxide derivative with similar NQO2 inhibitory potency, it is shown that the *N*-oxide moiety confers substantially reduced toxicity and reduced nuclear uptake and DNA binding.

Received: April 7, 2011

Published: August 22, 2011

Scheme 1. Preparation of Imidazoacridin-6-ones^a

^a (i) H_2SO_4 , HNO_3 , 70 °C, 1 h; (ii) *p*- R^1 -aniline, 24 h; (iii) $POCl_3$, 1,2-dichloroethane, 1 h, 90 °C; (iv) *N,N*-dimethylaniline/*N,N*-diethylaniline, DMF, reflux, 4 h; (v) Raney Ni, THF, 1 h, room temp; (vi) trimethyl orthoformate, reflux, 24 h; (vii) trimethyl orthoacetate, reflux, 24 h; (viii) *m*-CPBA, $CHCl_3$, 18 h.

Finally, it is demonstrated that the imidazoacridin-6-one containing the *N*-oxide is functionally active for inhibiting NQO2 in cells at nontoxic concentrations.

RESULTS AND DISCUSSION

Chemistry. Synthesis of a range of imidazoacridin-6-ones (Scheme 1), in which there are two loci for variation (positions 1 and 2), was carried out using an approach previously described by Cholody et al.¹⁹ A known property of these compounds is their ability to bind to DNA. Hence, part of the synthetic strategy was to reduce this potentially confounding effect by introducing an *N*-oxide moiety into the tertiary aminoalkyl side chains of these molecules.

Biochemical and Biological Evaluation. Figure 1 shows the general structure of the compounds evaluated here. All 19 compounds, 11 imidazoacridin-6-ones (designated 5) and 8 corresponding *N*-oxides (designated 6), were assayed for their ability to inhibit purified recombinant human NQO2 (Table 1). The IC_{50} values for these compounds were found to extend from 14 to 205 nM, with 6a1 being one of the most potent agents yet reported. Our previous work on imidazoacridin-6-ones as potential inhibitors of NQO2 was based on a substructure search following hierarchical screening of the NCI chemical database.¹¹ These compounds were supplied by the NCI, and by use of computational molecular docking, a reliable QSAR model was established. A number of the compounds were resynthesized for

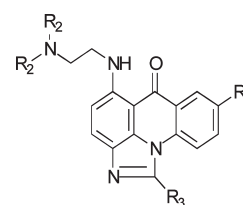


Figure 1. General structure of the imidazoacridin-6-ones.

the present work (5c1, 5e1, 5f1, 5c2, 5e2, 5f2), and generally there was no more than a 3-fold difference in enzyme inhibitory potency or toxicity when comparing the fresh stocks prepared here with compounds supplied by NCI (Table 1). The exception was 5c1, where the inhibitory potency was 7× lower for the NCI compound, although the toxicity against HCT116 cells was similar. As part of the screening of the NCI database we also identified triazoloacridin-6-ones as potential inhibitors of NQO2.¹² Although these compounds were around 10-fold less efficient as enzyme inhibitors than the imidazoacridin-6-ones, this study did illustrate that inclusion of an *N*-oxide moiety into the triazoloacridin-6-ones substantially reduced toxicity without compromising inhibitory potency. Introducing this functionality into these molecules also reduced DNA binding affinity and protein binding, both of which could potentially make the compounds more pharmacologically acceptable as inhibitors of NQO2. Hence, in

Table 1. Calculated Computational Binding Affinities (ΔG) for Ligands in the Active Site of NQO2 (1QR2 or 5a1 Crystal Structure), Their Experimental Enzyme Inhibitory Potency (IC_{50}), and Toxicity towards HCT116 Colon Cancer Cells after Exposure to Compounds for 24 or 96 h^a

compd	R ₁	R ₂	R ₃	IC ₅₀ (nM), NQO2	ΔG_{calcd} (kJ/mol)		toxicity IC ₅₀ (μM) at	
					1QR2	5a1	24 h	96 h
5a1	OCH ₃	CH ₃	H	59 ± 7	-49.8	-48.9	2.1 ± 0.35	0.51 ± 0.03
5b1	F	CH ₃	H	97 ± 8	-48.4	-48.2	2.9 ± 0.23	0.66 ± 0.03
5c1 (NSC645833)	H	CH ₃	H	115 ± 14, 830 ± 112 ^b	-47.5	-47.9	2.53 ± 0.35	0.60 ± 0.02
5e1 (NSC645808)	OH	CH ₃	H	83 ± 6, 296 ± 51 ^b	-48.7	-47.7	1.61 ± 0.18	0.37 ± 0.02, 1 ^b
5f1 (NSC645809)	OH	CH ₂ CH ₃	H	126 ± 81, 148 ± 4 ^b	-49.0	-47.1	4.16 ± 0.35	1.14 ± 0.41, 0.77 ^b
5a2	OCH ₃	CH ₃	CH ₃	46 ± 11	-50.8	-48.9	1.86 ± 0.35	0.46 ± 0.16
5b2	F	CH ₃	CH ₃	83 ± 11	-50.4	-47.9	2.11 ± 0.19	0.51 ± 0.11
5c2 (NSC645834)	H	CH ₃	CH ₃	90 ± 11, 323 ± 100 ^b	-49.8	-47.8	1.94 ± 0.68, 2.27 ^b	0.50 ± 0.16, 0.460 ^b
5d2	Br	CH ₃	CH ₃	74 ± 9	-49.5	-48.7	1.91 ± 0.10	0.44 ± 0.11
5e2 (NSC637991)	OH	CH ₃	CH ₃	90 ± 11, 50 ± 6 ^b	-50.3	-48.1	3.01 ± 1.32	0.95 ± 0.18, 0.650 ^b
5f2 (NSC637992)	OH	CH ₂ CH ₃	CH ₃	54 ± 8, 16 ± 1.5 ^b	-51.4	-48.8	5.46 ± 1.67	0.93 ± 0.31, 3 ^b
6a1	OCH ₃	CH ₃	H	14 ± 4	-51.8	-49.4	40.3 ± 2.1	12.8 ± 2.8
6b1	F	CH ₃	H	205 ± 18	-46.2	-46.1	40.3 ± 3.2	17.3 ± 3.1
6c1	H	CH ₃	H	96 ± 5	-49.7	-47.7	41.0 ± 3.0	12.1 ± 1.9
6e1	OH	CH ₃	H	42 ± 6	-50.3	-48.6	38.7 ± 11	19.7 ± 1.8
6a2	OCH ₃	CH ₃	CH ₃	73 ± 7	-50.5	-48	58.2 ± 1.8	11.4 ± 1.4
6b2	F	CH ₃	CH ₃	97 ± 6	-49.2	-47.5	31.0 ± 1.1	9.2 ± 0.3
6c2	H	CH ₃	CH ₃	56 ± 10	-50.5	-48.7	34.9 ± 1.8	16.1 ± 0.7
6d2	Br	CH ₃	CH ₃	47 ± 12	-51.2	-48.4	49.0 ± 1.8	10.6 ± 1.0

^a Values are given with \pm SD. ^b Data from ref 13.

Table 2. Activity of NQO2 in Breast Cancer Cell Lines ($[(\text{nmol of DCPIP Reduced})/\text{min}]/(\text{mg of Protein})$) and Their Sensitivity to the Imidazoacridin-6-ones^a

toxicity	cell line						
	MCF-7	SKBr3	BT20	BT474	MDA 468	MDA 231	T47D
5a1	0.41 ± 0.02	1.02 ± 0.09	0.88 ± 0.09	1.04 ± 0.10	1.95 ± 0.15	0.93 ± 0.05	0.34 ± 0.05
6a1	4.61 ± 0.28	9.53 ± 0.35	6.3 ± 0.3	7.67 ± 0.21	6.15 ± 0.23	4.42 ± 0.24	3.48 ± 0.18
5c1	0.43 ± 0.06	1.9 ± 0.10	0.99 ± 0.04	1.11 ± 0.14	1.12 ± 0.10	1.02 ± 0.03	0.44 ± 0.02
6c1	7.97 ± 0.25	10.47 ± 0.75	7.42 ± 0.49	5.99 ± 0.42	9.42 ± 0.33	8.84 ± 0.3	7.35 ± 0.31
NQO2 activity	8 ± 1.10	286 ± 25	11 ± 5.5	10 ± 7	28 ± 10	292 ± 28	468 ± 132

^a The compounds designated 5 are parent compounds, and those designated 6 are the corresponding *N*-oxides. Values given are with \pm SD.

the current study we included synthesis of *N*-oxide derivatives of the imidazoacridin-6-ones (designated 6). Clearly, the introduction of the *N*-oxide group shows little or no systematic effect on enzyme inhibitory potency (Table 1). However, it is apparent that the toxicity of the *N*-oxides toward HCT116 colon cancer cells is consistently around 20-fold less compared to their parent (5) analogues. The HCT116 cells contain significant levels of NQO2 ((493 nmol of DCPIP reduced/min)/(mg of protein)).¹² Therefore, in order to confirm this toxicity trend and also determine whether there was likely to be a dependence on NQO2 for toxicity, two pairs of compounds (5a1 and 6a1, and

5c1 and 6c1) were evaluated in a panel of seven breast cancer cell lines with varying NQO2 activities (from 8 to 468 (nmol of DCPIP reduced/min)/(mg of protein); Table 2). In each cell line, the *N*-oxide always showed lower toxicity than its parent compound. Further, there is clearly no relationship between the level of cellular NQO2 activity and toxicity. Consistent with our previous observations,¹² the inclusion of the *N*-oxide group decreases the ability of the compounds to interact with DNA. This is shown by the DNA melting curves in Figure 2. The control T_m in these experiments was 85 °C; in the presence of the parent imidazoacridin-6-one, 5a1, this increases to 88.6 °C.

In contrast, the *N*-oxide **6a1** shows little if any increase in melting temperature. In light of these differences in DNA binding affinity, the subcellular distribution of the imidazoacridin-6-ones was explored by fluorescent imaging. MDA468 cells were treated with $5\ \mu\text{M}$ **5a1** or $25\ \mu\text{M}$ **6a1** (to reflect the differences in toxicity of the two compounds), then harvested and treated with phalloidin to visualize the cellular architecture. Figure 3 shows the fluorescent images of cells treated with the two compounds. Nuclei of cells treated with **5a1** are clearly visible which is consistent with the DNA binding affinity of this compound. In contrast, little nuclear binding is observed with **6a1**, even though it is present at a 5-fold higher concentration; however, a high level of cytoplasmic fluorescence is observed. Interestingly, this could point to a different mechanism of toxicity for the two classes of compound. This difference in nuclear uptake/binding is recapitulated in a second cell line (HT29 colon cancer cells), and this is given in the Supporting Information (Figure 1).

Another significant difference between the parent imidazoacridin-6-ones and their *N*-oxide derivatives is their apparent protein binding ability. This is determined indirectly by measuring the ability of the compounds to inhibit NQO2 in the presence or absence of $2\ \mu\text{M}$ bovine serum albumin (BSA). Two pairs of compounds were evaluated (**5a1/6a1** and **5c1/6c1**). For **6a1** the presence of BSA reduced enzyme inhibitory potency from 14 to

98 nM (a 7-fold change). In contrast, BSA reduced the activity of **5a1** from 59 to 3200 nM (a 54-fold change). Similarly, the fold change for the *N*-oxide, **6c1**, was 6.5, whereas for the parent compound, **5c1**, the change was 38. Thus, it is likely that the *N*-oxide derivatives are likely to be less protein bound and therefore may have some advantage for probing for the functionality of NQO2 in cells. To test this, we evaluated the ability of **6a1** to protect MDA468 cells against the cytotoxic effects of 5--(aziridin-1-yl)-2,4-dinitrobenzamide, **7** (CB1954).²⁰ This agent is exquisitely dependent upon the presence of NQO2 in human cells for it to be metabolically activated to give a potent cytotoxin.²⁰ Thus, inhibition of the toxicity of **7** in air can be regarded as a surrogate measure of the inhibitory potency of the imidazoacridin-6-ones in cells. Figure 4 shows the toxicity of **7** in MDA468 cells treated for 3 h with varying concentrations of **6a1** in the presence of $100\ \mu\text{M}$ *N*-ribosylnicotinamide (NRH), the cofactor necessary to facilitate metabolic activation by NQO2. It is clear that the presence of **6a1** can inhibit the toxicity of **7** and that inhibition occurs at concentrations of **6a1** that are nontoxic. Hence, this provides evidence for the first time that an agent like **6a1**, an *N*-oxide substituted imidazoacridin-6-one, can inhibit NQO2 in cells and therefore can be used as a pharmacological probe for the function of this enzyme.

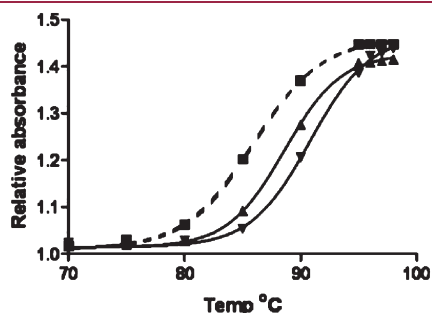


Figure 2. DNA melting curves for calf thymus DNA ($10\ \mu\text{M}$) in the presence of $10\ \mu\text{M}$ **5a1** or **6a1**. Experiments were repeated on three separate occasions and values of $T_m \pm \text{SD}$ are 85.0 and 85.0 for control and **6a1**, respectively (three experiments giving identical results), and 88.6 ± 0.5 for **5a1**. $10\ \mu\text{M}$ adriamycin is used as a positive control in these experiments ($T_m = 90.8 \pm 0.9$).

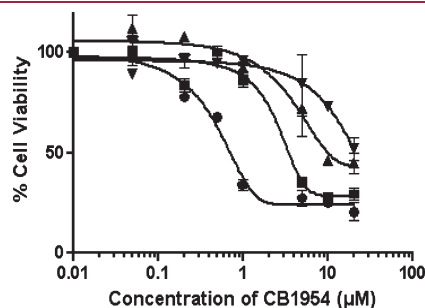
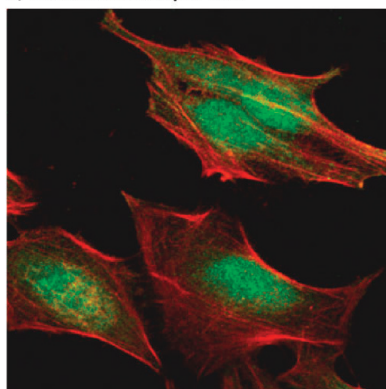


Figure 4. Functional activity of **6a1** as an inhibitor of NQO2 in MDA468 cells. The activity of NQO2 in cells is shown by the ability of the enzyme to activate **7** (CB1954) to give a cytotoxic metabolite. Cells were treated with $10\ \mu\text{M}$ **7** and varying concentrations of **6a1**: (●) **7** alone; (■) **7** plus $10\ \mu\text{M}$ **6a1**; (▲) **7** plus $100\ \mu\text{M}$ **6a1**; (▼) **7** plus $500\ \mu\text{M}$ **6a1**.

A; Localisation of $5\ \mu\text{M}$ 5a1



B; Localisation of $25\ \mu\text{M}$ 6a1

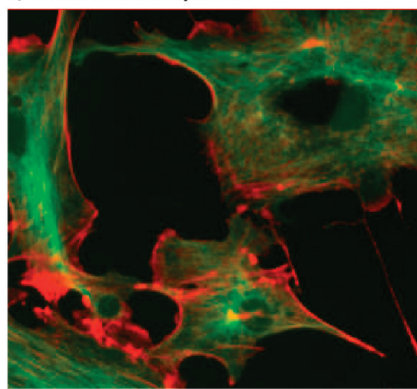


Figure 3. Subcellular localization of **5a1** and **6a1** as revealed by fluorescence microscopy. MDA468 cells exposed to $5\ \mu\text{M}$ **5a1** (A) and $25\ \mu\text{M}$ **6a1** (B). Red staining indicates the binding of phalloidin to β -actin which illuminates cellular architecture. Nuclear binding of **5a1** is apparent in part A, whereas much lower fluorescence in the nucleus is observed for **6a1** in part B.

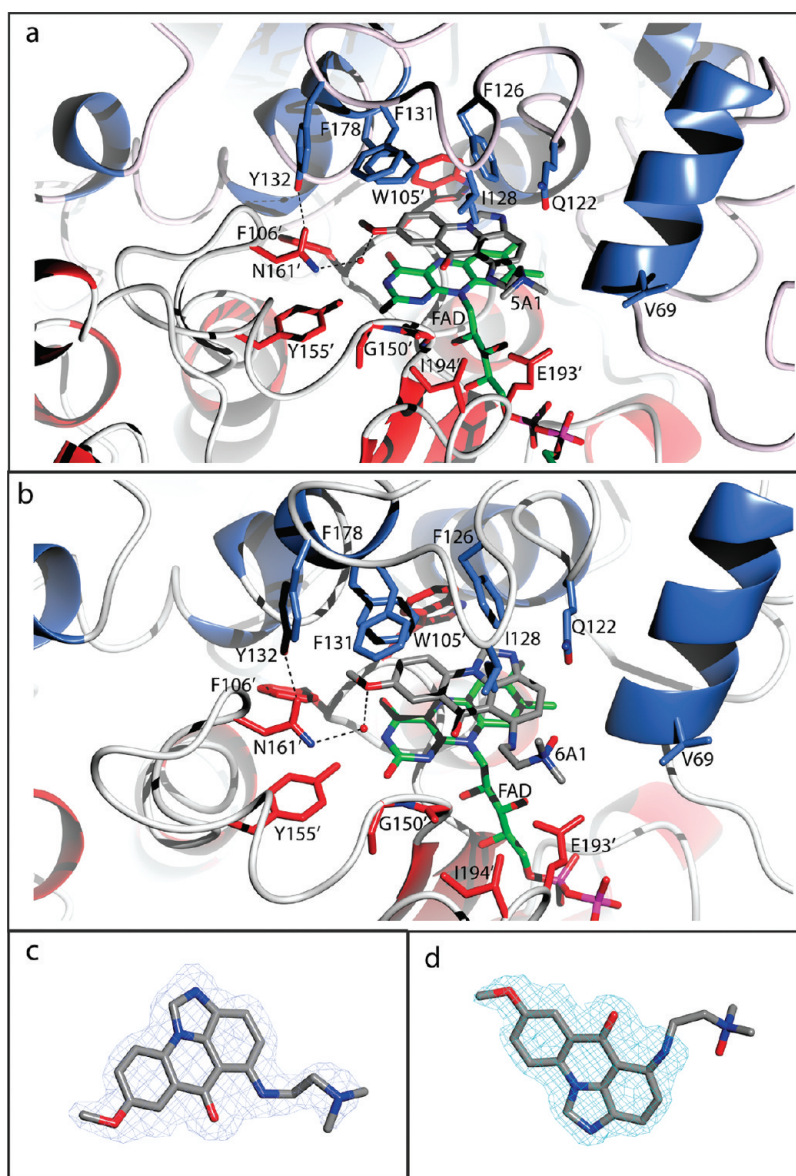


Figure 5. X-ray crystal structures of the imidazoacridin-6-one ligands **5a1** and **6a1**, showing detailed views of (a) **5a1** and (b) **6a1** bound in the NQO2 active site. The individual monomers and key active site residues are colored red and blue. The cofactor FAD is shown in green with hydrogen bonds indicated by black dotted lines. Parts c and d show the ligands **5a1** and **6a1** in omitted $2F_o - F_c$ electron density contoured at 1.2σ .

Molecular Modeling and Crystallography. The imidazoacridin-6-ones were docked into the active site of NQO2 using the crystal structure of the apoenzyme with bound FAD as a starting model (PDB code 1QR2, resolution at 2 \AA).²¹ The **5** series were docked in their protonated form. As previously described,¹³ the docking calculations predicted only one energetically favorable binding mode for this series of compounds (see Supporting Information Figure 2). After docking, the calculated binding affinities were compared with the newly measured experimental IC_{50} values for enzyme inhibition (see Supporting Information Figure 3) and a correlation coefficient of $R^2 = 0.82$ was established.

To further investigate the binding of imidazoacridin-6-one ligands to NQO2, **5a1** and the corresponding *N*-oxide **6a1** were cocrystallized with the enzyme (Figure 5). Both NQO2–ligand complexes crystallized in the space group $P2_12_12_1$, forming a single dimer in the asymmetric unit. While both imidazoacridin-6-one ligands are well-defined in the electron density and can be

placed unambiguously, the *N*-oxide moiety of **6a1** appears disordered and was placed to match that of **5a1**.

The dimerization of NQO2 is functionally critical to its activity, with the resulting interface forming two active sites made up of residues from both monomers. The **5a1** and **6a1** imidazoacridin-6-one ligands interact primarily through hydrophobic interactions with residues from both monomers and stacking interactions via the conjugate ring system of FAD. Figure 5 shows that the isoalloxazine ring of FAD provides the floor of the active site and stacks with the imidazoacridin-6-one moiety of both **5a1** and **6a1**. Hydrophobic residues F126, F131, and Y132 form the top of the active site, while W105' (primes denote residues from the other NQO2 monomer) sits at the back of the binding pocket and forms a hydrophobic interaction with the ring system of both **5a1** and **6a1**. Q122 and E193' form an electrostatic environment for the tail of **5a1** and the *N*-oxide moiety of **6a1**. The apparent disorder seen in the *N*-oxide tail of **6a1** is likely due to the

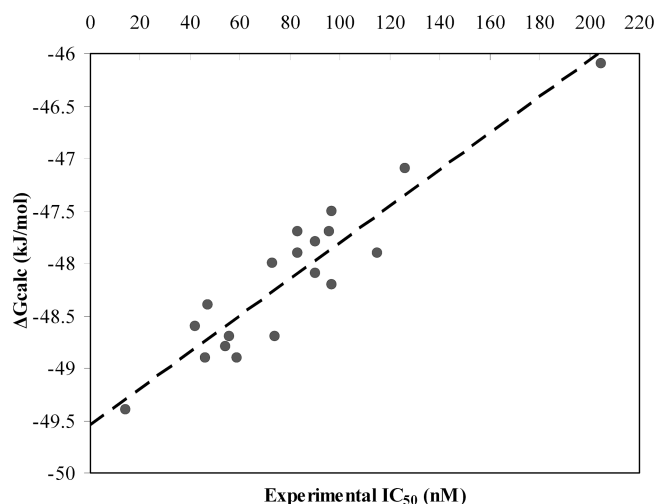


Figure 6. Relationship between the calculated binding affinity (ΔG) of the imidazoacridin-6-ones to NQO2 using the **5a1** crystal structure and their ability to act as inhibitors of the enzyme (IC_{50}).

predominately negative charge from the single bonded oxygen that would repel the negatively charged side chain of Q122. These repulsive effects would allow the **6a1** tail moiety to explore more of the binding cavity leading to numerous low occupancy conformations and ultimately the loss of any definitive high occupancy site. Although there are no direct H-bonds to any main chain or side chain residues, the OMe group of both ligands forms a water-mediated hydrogen bond contact with N161. The side chain of N161 is held in place via a hydrogen bond to the OH of Y132. A similar water-mediated interaction to N161 is also seen in the imatinib bound structure of NQO2,²² which might suggest a conserved mode of binding for some of these inhibitors.

Molecular docking of **5a1** and **6a1** initially suggested that these ligands interacted with NQO2 in an alternative orientation with the tail moiety making a direct hydrogen bond contact with the ND2 of N161. The removal of all water molecules prior to modeling simulations may explain these differences. To investigate this further, the imidazoacridine-6-ones were docked into the active site of the **5a1** crystal structure and the conserved crystal water was retained. The docked orientation of **5a1** and **6a1** was superimposed onto the crystal ligands with a root-mean-square deviation (rmsd) of 0.98 and 1.12, respectively (see Supporting Information Figure 4). Interestingly, the docking calculations suggest that ligands with a methoxy (**5a1**, **5a2**, **6a1**, and **6a2**) and hydroxy (**5e1**, **5f1**, **5e2**, **5f2**, and **6e1**) substituent at the R1 position bind in a similar orientation to the crystal pose. However, ligands with a halide substituent (**5b1**, **5b2**, **5c2**, **5d2**, **6b1**, **6b2**, and **6d2**) and hydrogen (**5c1**, **5c2**, **6c1**, and **6c2**) at R1 bind in an alternative orientation (180° rotation about the Y axis) compared to the crystal pose. The tail moiety forms a hydrogen bond with either G149 or a water mediated hydrogen bond with N161 (see Supporting Information Figure 5 for examples of **5b1** and **6b1**). The calculated binding affinities derived from docking into the crystal structure of **5a1** are shown in Table 1 and have been plotted against the experimental IC_{50} values in Figure 6, giving a correlation coefficient of 0.87. Since it is not clear how easily the conserved water molecule would be displaced upon ligand binding, any future modeling simulations with NQO2 inhibitors should perhaps take into account this ordered water molecule during its calculations.

CONCLUSIONS

In this work it has been shown that imidazoacridin-6-ones can be potent nanomolar inhibitors of recombinant human NQO2 and further, one of the *N*-oxides, **6a1**, shows the ability to inhibit the enzymatic function of NQO2 in cells. Compounds representative of a variety of structural classes have been shown to inhibit isolated NQO2,^{7–9,11–16} but this is the first demonstration that a novel inhibitor of NQO2 can be functionally active as an inhibitor in cells at nontoxic concentrations. Since NQO2 has been shown to have other properties in cells such as acting as a chaperone protein, the development of agents like **6a1** provides a pharmacological basis to study these, and other, cellular functions of the enzyme.

EXPERIMENTAL SECTION

Chemistry. Chemicals were purchased from Aldrich Chemical Co. Column chromatography was carried out using silica gel grade 60 (230–400 mesh). The ^1H and ^{13}C NMR spectra were recorded on Bruker Avance spectrometers operating at 300, 400, and 500 MHz. Chemical shifts are reported as δ_{H} or δ_{C} in parts per million (ppm) downfield from tetramethylsilane (TMS) for samples run in CDCl_3 . Mass spectra were carried out at the School of Chemistry, University of Manchester, U.K., using a Micromas Trio 2000 (CI, EI, FAB) and Micromas Platform 2 (electrospray). CI mass spectra were recorded using ammonia as a carrier gas. Melting points were determined using a Gallenkamp MPD.350.BM2.5 machine and remain uncorrected. The purity of all compounds was judged to be greater than or equal to 95% based on assessment of TLC, melting point, and ^1H NMR data.

Synthesis of 2,6-Dichloro-3-nitrobenzoic Acid. 2,6-Dichlorobenzoic acid (5.00 g, 26.2 mmol) was added gradually to concentrated H_2SO_4 (200 mL) with stirring, and the mixture was warmed to 50°C until all solid had completely dissolved. Concentrated HNO_3 (2.0 mL) was added gradually, and the mixture was stirred for 1 h. The resulting solution was allowed to cool before it was poured onto ice (800 g) with stirring. The solution was kept cool until crystallization was complete, and the resulting solid was collected by filtration to give 2,6-dichloro-3-nitrobenzoic acid (5.87 g, 95%). Mp $143\text{--}144^\circ\text{C}$; $\nu_{\text{max}}/\text{cm}^{-1}$ 3380w (O–H), 2884w (C–H), 1671s (C=O), 1644s; δ_{H} (500 MHz, CDCl_3) 7.92 (1H, d, *J* 8.8, C(4)H), 7.55 (1H, d, *J* 8.8, C(5)H), 6.84 (1H, br s, OH); δ_{C} (100 MHz, CDCl_3) 166.6 (q), 146.6 (q), 135.9 (q), 135.4 (q), 128.9 (q), 126.9 (C(4)H), 125.5 (C(5)H); *m/z* (–ES) 237.0 (6, $[\text{M} - \text{H}]^-$, $^{35}\text{Cl}^{37}\text{Cl}$), 235.0 (10, $[\text{M} - \text{H}]^-$, $^{35}\text{Cl}^{35}\text{Cl}$), 194 (15, $[\text{M} - \text{NO}_2]^-$, $^{37}\text{Cl}^{37}\text{Cl}$), 192 (70, $[\text{M} - \text{NO}_2]^-$, $^{35}\text{Cl}^{37}\text{Cl}$), 190 (100, $[\text{M} - \text{NO}_2]^-$, $^{35}\text{Cl}^{35}\text{Cl}$); 234.9454 ($[\text{M} - \text{H}]^-$, $^{35}\text{Cl}^{35}\text{Cl}$) found by –ES, required 234.9445, error 4.0 ppm.

Synthesis of 2-(4-Methoxyphenylamino)-6-chloro-3-nitrobenzoic Acid (1a). A solution of 4-methoxyaniline (0.700 g, 5.68 mmol) in *N,N*-dimethylaniline (1.5 mL) was added to a flask containing 2,6-dichloro-3-nitrobenzoic acid (1.00 g, 4.24 mmol) in *N,N*-dimethylaniline (3.0 mL). The mixture was warmed with stirring under nitrogen for 18 h. Once cooled, it was diluted with CHCl_3 (20 mL), extracted with 1 M NaOH (20 mL), and washed twice with 1 M NaOH (2×10 mL). The combined aqueous extracts were acidified with dilute HCl to pH 3, resulting in formation of a yellow precipitate which was collected by filtration and dried to give **1a** (0.779 g, 57%). Mp $211\text{--}213^\circ\text{C}$; $\nu_{\text{max}}/\text{cm}^{-1}$ 3297w (N–H), 2848w (C–H), 1698s (C=O), 1589s, 1574s, 1510s (C=C); δ_{H} (300 MHz, $\text{DMSO}-d_6$) 8.69 (1H, s, NH), 8.04 (1H, d, *J* 8.9, C(4)H), 7.17 (1H, d, *J* 8.9, C(5)H), 6.91 (2H, d, *J* 8.9, C(10)H, C(12)H), 6.79 (2H, d, *J* 8.9, C(9)H, C(13)H), 3.70 (3H, s, C(14)H₃); δ_{C} (75 MHz, $\text{DMSO}-d_6$) 165.0 (q), 155.6 (q), 153.3 (q), 138.4 (q), 136.5 (q), 134.7 (q), 134.0 (q), 127.6 (C(4)H), 122.6 (CH, Ph), 120.9 (C(5)H), 114.0 (CH, Ph), 55.2 (OCH₃); *m/z* (–ES) 323

(10, $[M - H]^-$, ^{37}Cl), 321 (30, $[M - H]^-$, ^{35}Cl); 321.0290 ($[M - H]^-$) found by $-ES$, required 321.0278, error 3.7 ppm.

Synthesis of 2-(4-Fluorophenylamino)-6-chloro-3-nitrobenzoic Acid (1b). A solution of 4-fluoroaniline (0.54 mL, 5.68 mmol) in *N,N*-dimethylaniline (1.5 mL) was added to a flask containing 2,6-dichloro-3-nitrobenzoic acid (1.00 g, 4.24 mmol) in *N,N*-dimethylaniline (3.0 mL). The mixture was warmed with stirring under nitrogen for 18 h. Once cooled, it was diluted with CHCl_3 (20 mL), extracted with 1 M NaOH (20 mL), and washed twice with 1 M NaOH (2×10 mL). The combined aqueous extracts were acidified with dilute HCl to pH 3, resulting in formation of a yellow precipitate which was collected by filtration and dried to give **1b** (0.786 g, 60%). Mp 176.5–177.0 °C; $\nu_{\text{max}}/\text{cm}^{-1}$ 3348w (N–H), 2980br (O–H), 2881w, (C–H), 1704s (C=O), 1588s, 1569s, 1530m, 1504s (C=C); δ_{H} (300 MHz, DMSO- d_6) 10.73 (1H, s, C(7)O₂H), 8.57 (1H, s, NH), 8.05 (1H, d, J 8.9, C(4)H), 7.35 (1H, d, J 8.9, C(5)H), 7.02 (2H, app t, J 8.8, C(10)H, C(12)H), 6.88 (2H, dd, J 8.7, 4.8, C(9)H, C(13)H); δ_{C} (75 MHz, DMSO- d_6) 165.1 (q), 157.7 (d, J 237.9, C(11)F), 140.9 (q), 139.2 (q), 136.5 (q), 135.8 (q), 131.1 (q), 127.5 (C(4)H), 123.1 (C(5)H), 120.6 (d, J 8.1, C(9)H, C(13)H), 115.3 (d, J 22.7, C(10)H, C(12)H); δ_{F} (376 MHz, DMSO- d_6) –121.60, –121.52 (m); m/z ($-ES$) 311 (10, $[M - H]^-$, ^{37}Cl), 309 (30, $[M - H]^-$, ^{35}Cl), 309.0090 ($[M - H]^-$) found by $-ES$, required 309.0084, error 2.0 ppm.

Synthesis of 6-Chloro-3-nitro-2-(phenylamino)benzoic Acid (1c). A solution of aniline (0.879 g, 8.47 mmol) in *N,N*-dimethylaniline (50 mL) was added to a flask containing 2,6-dichloro-3-nitrobenzoic acid (1.00 g, 4.23 mmol) in *N,N*-dimethylaniline (50 mL). The mixture was warmed with stirring under nitrogen for 18 h. Once cooled, it was diluted with CHCl_3 (100 mL), extracted with 1 M NaOH (50 mL), and washed twice with 1 M NaOH (2×30 mL). The combined aqueous extracts were acidified with dilute HCl to pH 3, resulting in formation of a yellow precipitate which was collected by filtration and dried to give **1c** (0.552 g, 45%). Mp 203–205 °C (lit., 199–204 °C); $\nu_{\text{max}}/\text{cm}^{-1}$ 3333w (N–H), 3040w (C–H), 1704s (C=O), 1583s, 1568s; δ_{H} (500 MHz, DMSO- d_6) 8.47 (1H, s, NH), 8.02 (1H, d, J 8.8, C(4)H), 7.41 (1H, d, J 8.8, C(5)H), 7.14 (2H, app t, J 7.9 C(10)H, C(12)H), 6.85 (1H, app t, J 7.4, C(9)H, C(11)H), 6.77 (2H, d, J 7.6, C(9)H, C(13)H); δ_{C} (125 MHz, DMSO- d_6) 165.1 (q), 143.4 (q), 142.1 (q), 135.3 (C(4)H), 132.5 (q), 129.0 (q), 128.6 (C(10)H, C(12)H), 127.7 (C(11)H), 124.1 (q), 121.0 (C(9), C(13)H), 116.9 (C(5)H); m/z ($-ES$) 293 (8, $[M - H]^-$, ^{37}Cl), 291 (24, $[M - H]^-$, ^{35}Cl), 249 (41, M – CO₂H, ^{37}Cl), 247 (100, M – CO₂H, ^{37}Cl); 291.0178 ($[M - H]^-$) found by $-ES$, required 291.0178, error 0.0 ppm.

Synthesis of 2-(4-Bromophenylamino)-6-chloro-3-nitrobenzoic Acid (1d). 4-Bromoaniline (7.29 g, 42.4 mmol, 5 equiv) was heated to 110 °C until completely melted. 2,6-Dichloro-3-nitrobenzoic acid (2.00 g, 8.47 mmol, 1 equiv) was then added in small portions over 20 min with stirring. Heating was continued, and after 3 h a solid mass had formed which was kept at 110 °C for a further 4 h. Once cooled to room temperature, this solid was thoroughly crushed in 2 M NaOH (30 mL) and the mixture left to stir for 30 min. Unreacted 4-bromoaniline was collected by filtration and washed once with 2 M NaOH (5 mL) and twice with water (2×5 mL). The filtrate was then acidified with dilute HCl to pH 3, which resulted in formation of a yellow precipitate which was collected by filtration and dried to give **1d** (1.89 g, 60%) as a yellow powder. Mp 198.8–202.0 °C; $\nu_{\text{max}}/\text{cm}^{-1}$ 3305w (N–H), 3090w, 2818m (C–H), 1703s (C=O), 1596s, 1574s, 1528m; δ_{H} (500 MHz, DMSO- d_6) 13.87 (1H, s, C(7)O₂H), 8.54 (1H, s, NH), 8.06 (1H, d, J 8.9, C(4)H), 7.51 (1H, d, J 8.9, C(5)H), 7.30 (2H, d, J 8.8, C(10)H, C(12)H), 6.71 (2H, d, J 8.8, C(9)H, C(13)H); δ_{C} (125 MHz, DMSO- d_6) 165.0 (q), 143.4 (q), 143.0 (q), 135.2 (q), 134.5 (q), 133.5 (q), 131.5 (C(10)H, C(12)H), 127.3 (C(4)H), 125.2 (C(5)H), 118.7 (C(9)H, C(13)H), 112.0 (q, C(11)); m/z ($-ES$) 373 (25, $[M - H]^-$, $^{37}\text{Cl}^{81}\text{Br}$), 371 (100, $[M - H]^-$, $^{37}\text{Cl}^{79}\text{Br}$,

$^{35}\text{Cl}^{81}\text{Br}$), 369 (80, $[M - H]^-$, $^{35}\text{Cl}^{79}\text{Br}$); 368.9282 ($[M - H]^-$) found by $-ES$, required 368.9283, error 0.3 ppm.

Synthesis of 2-(4-(Benzyloxy)phenylamino)-6-chloro-3-nitrobenzoic Acid (1e). A solution of 4-benzyloxyaniline (2.03 g, 10.2 mmol) in *N,N*-dimethylaniline (3.0 mL) was added to a flask containing 2,6-dichloro-3-nitrobenzoic acid (2.00 g, 8.47 mmol) in *N,N*-dimethylaniline (6.0 mL). The mixture was warmed with stirring under nitrogen for 18 h. Once cooled, it was diluted with CHCl_3 (40 mL), extracted with 1 M NaOH (40 mL), and washed twice with 1 M NaOH (2×20 mL). The combined aqueous extracts were acidified with dilute HCl to pH 3, resulting in formation of a yellow precipitate which was collected by filtration and dried to give **1e** (1.27 g, 38%). Mp 271.5–271.8 °C; $\nu_{\text{max}}/\text{cm}^{-1}$ 3314m (N–H), 3037m (C–H), 16577s (C=O), 1618s, 1594s; δ_{H} (300 MHz, DMSO- d_6) 9.18 (1H, s, NH), 7.62 (1H, d, J 8.9, C(4)H), 7.45–7.43 (5H, m, Ph), 6.95 (1H, d, J 8.9, C(5)H), 6.85 (2H, d, J 8.6, C(10)H, C(12)H), 6.69 (2H, d, J 8.6, C(9)H, C(13)H), 5.00 (2H, s, CH₂); δ_{C} (75 MHz, DMSO- d_6) 165.3 (q), 153.6 (q), 137.3 (q), 137.2 (q), 136.2 (q), 135.8 (q), 135.6 (q), 135.2 (q), 128.4 (CH), 127.7 (CH), 127.5 (CH), 124.1 (C(4)H), 120.6 (C(5)H), 118.2 (C(9)H, C(13)H), 115.2 (C(10)H, C(12)H), 69.5 (CH₂); m/z ($-ES$) 397 (100, $[M - H]^-$); 397.0593 ($[M - H]^-$) found by $-ES$, required 397.0596, error 0.8 ppm.

Synthesis of 1-Chloro-7-methoxy-4-nitroacridin-9(10H)-one (2a). A mixture of **1a** (248 mg, 0.80 mmol), POCl₃ (0.50 mL, 5.25 mmol), and *N,N*-dimethylaniline (0.16 mL) in 1,2-dichloroethane (25 mL) was heated under reflux for 2 h. The resulting red precipitate was collected by filtration, washed with ethanol (2.0 mL), and dried to give **2a** (186 mg, 58%) as red needles. Mp 263–264 °C; $\nu_{\text{max}}/\text{cm}^{-1}$ 3288m (N–H), 3113w, 2839w (C–H), 1644s (C=O), 1606s, 1589s, 1565s; δ_{H} (300 MHz, DMSO- d_6) 11.64 (1H, s, NH), 8.55 (1H, d, J 8.9, C(3)H), 8.02 (1H, d, J 9.1, C(5)H), 7.59 (1H, d, J 2.9, C(8)H), 7.47 (1H, dd, J 9.1, 2.9, C(6)H), 7.38 (1H, d, J 8.9, C(2)H), 3.16 (3H, s, C(14)H₃); m/z ($-ES$) 305 (35, $[M - H]^-$, ^{37}Cl), 303 (100, $[M - H]^-$, ^{35}Cl); (+ES) 329 (20, $[M + \text{Na}]^+$, ^{37}Cl), 327 (60, $[M + \text{Na}]^+$, ^{35}Cl); 303.0180 ($[M - H]^-$) found by $-ES$, required 303.0173, error 2.4 ppm.

Synthesis of 1-Chloro-7-fluoro-4-nitroacridin-9(10H)-one (2b). A mixture of **1b** (248 mg, 0.80 mmol), POCl₃ (0.50 mL, 5.25 mmol), and *N,N*-dimethylaniline (0.16 mL) in 1,2-dichloroethane (25 mL) was heated under reflux for 2 h. The resulting red precipitate was collected by filtration, washed with ethanol (2.0 mL), and dried to give **2b** (135 mg, 58%) as a red powder. Mp 269.5–271.0 °C; $\nu_{\text{max}}/\text{cm}^{-1}$ 3305m (N–H), 3078w (C–H), 1647s (C=O), 1624m, 1589s, 1569s, 1525w, 1484s; δ_{H} (300 MHz, DMSO- d_6) 11.68 (1H, NH), 8.55 (1H, d, J 8.8, C(3)H), 8.12 (1H, dd, J 8.9, 4.6, C(8)H), 7.82 (1H, dd, J 8.9, 3.0, C(5)H), 7.73 (1H, app dt, J 8.9, 3.0, C(6)H), 7.41 (1H, d, J 8.8, C(2)H); δ_{F} (376 MHz, DMSO- d_6) –117.65, –117.59 (m); m/z ($-ES$) 293 (35, $[M - H]^-$, ^{37}Cl), 291 (100, $[M - H]^-$, ^{35}Cl); (+ES) 317 (35, $[M + \text{Na}]^+$, ^{37}Cl), 315 (100, $[M + \text{Na}]^+$, ^{35}Cl); 314.9960 ($[M + \text{Na}]^+$) found by +ES, required 314.9943, error 5.3 ppm.

Synthesis of 1-Chloro-4-nitroacridin-9(10H)-one (2c). A mixture of **1c** (1.60 g, 5.47 mmol), POCl₃ (3.28 mL, 36 mmol), and *N,N*-dimethylaniline (0.16 mL) in dichloroethane (16 mL) was heated under reflux for 2 h. The resulting red precipitate was collected by filtration, washed with ethanol (2.0 mL), and dried to give **2c** as a red powder (1.23 g, 82%). Mp 248–249 °C; $\nu_{\text{max}}/\text{cm}^{-1}$ 3307m (N–H), 1644s (C=O); δ_{H} (500 MHz, DMSO- d_6) 11.47 (1H, s, NH), 8.55 (1H, d, J 8.8, C(3)H), 8.18 (1H, d, J 8.0, C(5)H), 7.99 (1H, d, J 8.2, C(8)H), 7.89–7.82 (1H, m, C(6)H), 7.40 (1H, d, J 8.8, C(2)H), 7.38–7.41 (1H, m, C(7)H); δ_{C} (100 MHz, DMSO- d_6) 174.9 (q), 141.8 (q), 138.4 (q), 137.0 (q), 133.9 (C(3)H), 130.1 (C(6)H), 125.6 (C(8)H), 123.2 (C(7)H), 122.5 (C(5)H), 121.8 (q), 118.6 (q), 118.3 (C(2)H), 99.2 (q); m/z ($-ES$) 275 (32, $[M - H]^-$, ^{37}Cl), 273 (100, $[M - H]^-$, ^{35}Cl); 297.0051 ($[M + \text{Na}]^+$) found by +ES, required 297.0054, error 2.7 ppm.

Synthesis of 7-Bromo-1-chloro-4-nitroacridin-9(10H)-one (2d). A mixture of **1d** (1.80 g, 4.84 mmol), POCl₃ (3.00 mL, 31.8 mmol), and *N,N*-dimethylaniline (0.14 mL) in 1,2-dichloroethane (14 mL) was heated under reflux for 1 h. The resulting red precipitate was collected by filtration, washed with 1,2-dichloroethane (2.0 mL), and dried to give **2d** as a bright red powder (1.61 g, 94%). Mp 310.0–310.8 °C; $\nu_{\max}/\text{cm}^{-1}$ 3291m (N–H), 3074m (C–H), 1658s (C=O), 1613, 1571s; δ_{H} (500 MHz, DMSO-*d*₆) 8.50 (1H, d, J 8.8, C(3)H), 8.24 (1H, s, C(8)H), 7.98 (1H, d, J 8.6, C(5)H), 7.93 (1H, d, J 8.6, C(6)H), 7.39 (1H, d, J 8.8, C(2)H); m/z (–ES) 355 (25, [M – H][–], ³⁷Cl⁸¹Br), 353 (100, [M – H][–], ³⁷Cl⁷⁹Br, ³⁵Cl⁸¹Br), 351 (80, [M – H][–], ³⁵Cl⁷⁹Br); (+ES) 378 (3, [M + Na]⁺, ³⁷Cl⁸¹Br), 376 (12, [M + Na]⁺, ³⁷Cl⁷⁹Br, ³⁵Cl⁸¹Br), 374 (9, [M + Na]⁺, ³⁵Cl⁷⁹Br); 350.9178 ([M – H][–]) found by –ES, required 350.9178, error 0.0 ppm.

Synthesis of 1-Chloro-7-hydroxy-4-nitroacridin-9(10H)-one (2e). A mixture of **1e** (1.20 g, 3.01 mmol) and POCl₃ (1.80 mL, 20 mmol) in dichloroethane (16 mL) was heated under reflux for 2 h. The resulting red precipitate was collected by filtration, washed with ethanol (2.0 mL), and dried to give **2e** as a red powder (0.841 g, 96%). Mp >400 °C; $\nu_{\max}/\text{cm}^{-1}$ 3326m (N–H), 3078m (C–H), 16308s (C=O), 1587, 1567s; δ_{H} (300 MHz, DMSO-*d*₆) 11.59 (1H, s, OH), 8.54 (1H, d, J 8.8, C(3)H), 7.92 (1H, d, J 9.0, C(5)H), 7.52 (1H, d, J 2.7, C(8)H), 7.36–7.30 (2H, m, C(6)H, C(2)H); m/z (–ES) 289 (100, [M – H][–]); 289.0015 ([M – H][–]) found by –ES, required 289.0011, error 1.1 ppm.

Synthesis of 1-(2-(Dimethylamino)ethylamino)-7-methoxy-4-nitroacridin-9(10H)-one (3a). *N,N*-Dimethylethylenediamine (1.09 mL, 10.0 mmol) was added to a suspension of **2a** (1.53 g, 5.00 mmol) in anhydrous DMF (5.0 mL), and the reaction mixture was heated to reflux for 4 h. Ethanol (10 mL) was added and the resulting yellow precipitate was collected by filtration and washed with ethanol (2.0 mL) to give **3a** (1.64 g, 92%). Mp 239.5–240.0 °C; $\nu_{\max}/\text{cm}^{-1}$ 3380m (N–H), 3068m, 2944m (C–H), 1666s (C=O), 1629s, 1606s, 1572s, 1543s; δ_{H} (500 MHz, CDCl₃) 12.69 (1H, s br, NH), 12.03 (1H, s br, NH), 8.46 (1H, d, J 9.8, C(3)H), 7.77 (1H, d, J 2.9, C(8)H), 7.41 (1H, d, J 8.8, C(5)H), 7.35 (1H, dd, J 8.8, 2.9, C(6)H), 6.36 (1H, d, J 9.8, C(2)H), 3.94 (3H, s, OCH₃), 3.54 (2H, app q, J 5.9, C(11)H₂), 2.74 (2H, t, J 6.3, C(12)H₂), 2.39 (6H, s, C(13)H₃, C(14)H₃); δ_{C} (75 MHz, CDCl₃) 179.3 (q), 158.0 (q), 156.5 (q), 139.8 (q), 133.9 (C(3)H), 132.7 (q), 124.8 (C(6)H), 123.6 (q), 121.1 (q), 119.3 (C(5)H), 105.3 (C(8)H), 104.3 (q), 102.2 (C(2)H), 57.5 (C(12)H₂), 55.8 (OCH₃), 45.5 (C(13)H₃, C(14)H₃), 41.2 (C(11)H₂); m/z (–ES) 355 (100, [M – H][–]); (+ES) 357 (100, [M + H]⁺); 357.1562 ([M + H]⁺) found by +ES, required 357.1557, error 1.3 ppm.

Synthesis of 1-(2-(Dimethylamino)ethylamino)-7-fluoro-4-nitroacridin-9(10H)-one (3b). *N,N*-Dimethylethylenediamine (1.09 mL, 10.0 mmol) was added to a suspension of **2b** (1.47 g, 5.00 mmol) in anhydrous DMF (5.0 mL), and the reaction mixture was heated to reflux for 4 h. Ethanol (10 mL) was added, and the resulting yellow precipitate was collected by filtration and washed with ethanol (2.0 mL) to give **3b** (1.43 g, 83%). Mp 236.5–237.0 °C; $\nu_{\max}/\text{cm}^{-1}$ 3196m (N–H), 3053m, 2947m (C–H), 1622s (C=O), 1602s; δ_{H} (500 MHz, CDCl₃) 12.70 (1H, s br, NH), 11.88 (1H, s br, NH), 8.46 (1H, d, J 9.8, C(3)H), 8.04 (1H, d, J 8.8, C(5)H), 7.46–7.47 (2H, m, C(6)H, C(8)H), 6.38 (1H, d, J 9.8, C(2)H), 3.52 (2H, app q, J 5.9, C(11)H₂), 2.72 (2H, t, J 6.3, C(12)H₂), 2.38 (6H, s, C(13)H₃, C(14)H₃); δ_{F} (376 MHz, DMSO-*d*₆) –117.81, –116.84 (m); m/z (–ES) 343 (100, [M – H][–]); (+ES) 367 (5, [M + Na]⁺), 345 (100, [M + H]⁺); 345.1364 ([M + H]⁺) found by +ES, required 345.1358, error 1.8 ppm.

Synthesis of 1-(2-(Dimethylamino)ethylamino)-4-nitroacridin-9(10H)-one (3c). *N,N*-Dimethylethylenediamine (1.09 mL, 10.0 mmol) was added to a suspension of **2c** (1.38 g, 5.00 mmol) in anhydrous DMF (5.0 mL), and the reaction mixture was heated to reflux for 4 h. Ethanol (10 mL) was added and the resulting yellow precipitate

was collected by filtration and washed with ethanol (2.0 mL) to give **3c** (1.10 g, 67%). Mp 211.0–211.8 °C; $\nu_{\max}/\text{cm}^{-1}$ 3233m (N–H), 3065m, 2977m, 2941m, 2862m, 2815m, 2768m (C–H), 1615s (C=O); δ_{H} (500 MHz, CDCl₃) 12.64 (1H, s br, NH), 11.96 (1H, s br, NH), 8.46 (1H, d, J 9.9, C(3)H), 8.40 (1H, d, J 8.2, C(8)H), 7.71 (1H, app t, J 7.2, C(6)H), 7.46 (1H, d, J 8.2, C(5)H), 7.38 (1H, app t, J 7.8, C(7)H), 6.38 (1H, d, J 9.9, C(2)H), 3.54 (2H, app q, J 5.9, C(11)H₂), 2.73 (2H, t, J 6.5, C(12)H₂), 2.38 (6H, s, C(13)H₃, C(14)H₃); δ_{C} (75 MHz, CDCl₃) 180.0 (q), 157.9 (q), 140.6 (q), 138.1 (q), 133.8 (C(3)H, C(6)H), 126.3 (C(8)H), 123.8 (C(7)H), 122.8 (q), 121.2 (q), 117.7 (C(5)H), 104.7 (q), 102.5 (C(2)H), 57.5 (C(11)H₂), 45.5 (C(13)H₃, C(14)H₃), 41.2 (C(12)H₂); m/z (–ES) 325 (100, [M – H][–]); (+ES) 327 (100, [M + H]⁺); 327.1463 ([M + H]⁺) found by +ES, required 327.1452, error 3.5 ppm.

Synthesis of 1-(2-(Dimethylamino)ethylamino)-7-bromo-4-nitroacridin-9(10H)-one (3d). *N,N*-Dimethylethylenediamine (0.54 mL, 5.00 mmol) was added to a suspension of **2d** (0.708 g, 2.00 mmol) in anhydrous DMF (6.0 mL), and the reaction mixture was heated to reflux for 4 h. Ethanol (10 mL) was added and the resulting yellow crystals were collected by filtration and washed with ethanol (2.0 mL) to give **3d** (792 mg, 98%). Mp 242.0–242.5 °C; $\nu_{\max}/\text{cm}^{-1}$ 3201m (N–H), 3065m, 2943w, 2859w (C–H), 1611s (C=O), 1592s, 1566s; δ_{H} (300 MHz, CDCl₃) 12.63 (1H, s br, NH), 11.82 (1H, s br, NH), 8.51 (1H, d, J 2.3, C(8)H), 8.44 (1H, d, J 10.0, C(3)H), 7.77 (1H, dd, J 8.7, 2.3, C(6)H), 7.34 (1H, d, J 8.7, C(5)H), 6.38 (1H, d, J 10.0, C(2)H), 3.52 (2H, app q, J 5.8, C(11)H₂), 2.73 (2H, t, J 6.3, C(12)H₂), 2.39 (6H, s, C(13)H₂, C(14)H₂); δ_{C} (75 MHz, CDCl₃) 178.6 (q), 157.7 (q), 140.5 (q), 136.8 (q), 136.8 (C(6)H), 134.0 (C(3)H), 128.9 (C(8)H), 123.9 (q), 121.2 (q), 119.4 (C(5)H), 117.1 (q), 104.7 (q), 102.8 (C(2)H), 57.4 (C(12)H₂), 45.5 (C(13)H₂, C(14)H₂), 41.2 (C(11)H₂); m/z (–ES) 405 (100, [M – H][–], ⁸¹Br), 403 (100, [M – H][–], ⁷⁹Br); (+ES) 407 (100, [M + H]⁺, ⁸¹Br), 405 (100, [M + H]⁺, ⁷⁹Br); 405.0558 ([M + H]⁺, ⁷⁹Br) found by +ES, required 405.0577, error 0.3 ppm.

Synthesis of 1-(2-(Dimethylamino)ethylamino)-7-hydroxy-4-nitroacridin-9(10H)-one (3e). *N,N*-Dimethylethylenediamine (1.09 mL, 10.0 mmol) was added to a suspension of **2e** (1.45 g, 5.00 mmol) in anhydrous DMF (5.0 mL), and the reaction mixture was heated to reflux for 4 h. Ethanol (10 mL) was added and the resulting precipitate was collected by filtration and washed with ethanol (2.0 mL) to give **3e** (1.60 g, 94%). Mp 215.0–215.8 °C; $\nu_{\max}/\text{cm}^{-1}$ 3204m (N–H), 3093m, 2946m (C–H), 1608s (C=O), 1568s, 1543s; δ_{H} (300 MHz, DMSO-*d*₆) 12.46 (1H, s br, NH), 11.95 (1H, s br, NH), 8.37 (1H, d, J 10.0, C(3)H), 7.86 (1H, d, J 9.0, C(5)H), 7.53 (1H, d, J 2.7, C(8)H), 7.28 (1H, dd, J 9.0, 2.7, C(6)H), 6.56 (1H, d, J 10.0, C(2)H), 3.54 (2H, app q, J 5.5, C(11)H₂), 2.61 (2H, t, J 6.0, C(12)H₂), 2.26 (6H, s, C(13)H₃, C(14)H₃); δ_{C} (75 MHz, DMSO-*d*₆) 178.2 (q), 157.4 (q), 154.2 (q), 139.1 (q), 133.3 (C(3)H), 131.4 (q), 123.8 (C(6)H), 123.2 (q), 120.5 (C(5)H), 120.1 (q), 107.8 (C(8)H), 103.1 (C(2)H), 102.7 (q), 57.0 (C(12)H₂), 45.0 (C(13)H₃, C(14)H₃), 36.3 (C(11)H₂); m/z (–ES) 341 (100, [M – H][–]); (+ES) 343 (100, [M + H]⁺); 343.1399 ([M + H]⁺) found by +ES, required 343.1401, error 0.7 ppm.

Synthesis of 1-(2-(Diethylamino)ethylamino)-7-hydroxy-4-nitroacridin-9(10H)-one (3f). *N,N*-Diethylethylenediamine (1.16 mL, 10.0 mmol) was added to a suspension of **2e** (1.45 g, 5.00 mmol) in anhydrous DMF (5.0 mL), and the reaction mixture was heated to reflux for 4 h. Ethanol (10 mL) was added and the resulting yellow precipitate was collected by filtration and washed with ethanol (2.0 mL) to give **3f** (1.68 g, 91%). Mp 218–220 °C; $\nu_{\max}/\text{cm}^{-1}$ 3216m (N–H), 2969m, 2808m (C–H), 1599s (C=O), 1548s; δ_{H} (300 MHz, DMSO-*d*₆) 12.46 (1H, s, NH), 11.97 (1H, s br, NH), 9.93 (1H, s, OH), 8.36 (1H, d, J 10.0, C(3)H), 7.85 (1H, d, J 9.0, C(5)H), 7.55 (1H, d, J 2.7, C(8)H), 7.28 (1H, dd, J 9.0, 2.7, C(6)H), 6.55 (1H, d, J 10.0, C(2)H), 3.50 (2H, app q, J 5.7,

C(11)H₂), 2.73 (2H, t, 5.7, C(12)H₂), 2.58 (4H, q, J 7.1, 2 × CH₂), 1.02 (6H, t, J 7.1, 2 × CH₃); δ_C (75 MHz, DMSO-*d*₆) 178.2 (q), 157.5 (q), 154.2 (q), 139.3 (q), 133.3 (C(3)H), 131.5 (q), 129.5 (q), 123.9 (C(6)H), 120.6 (C(5)H), 120.1 (q), 107.8 (C(8)H), 103.2 (C(2)H), 102.9 (q), 50.5 (C(12)H₂), 40.9 (C(11)H₂), 46.3 (CH₂), 11.7 (CH₃); *m/z* (−ES) 369 (100, [M − H][−]); (+ES) 393 (100, [M + Na]⁺), 371 (50, [M + H]⁺); 371.1712 ([M + H]⁺) found by +ES, required 371.1714, error 0.6 ppm.

Synthesis of 4-Amino-1-(2-(dimethylamino)ethylamino)-7-methoxyacridin-9(10*H*)-one Hydrochloride (4a). Raney Ni (750 mg) was added to a suspension of 3a (1.07 g, 3.00 mmol) and hydrazine monohydrate (0.6 mL) in THF (15 mL), and the reaction mixture was stirred for 1 h. The resulting solution was filtered through Celite and washed with THF (2.0 mL). The filtrate was treated with concentrated HCl to pH 3 and stirred for 30 min. The resulting brown precipitate was filtered and purified by recrystallization from MeOH–dioxane (9:1) (acidified with HCl to ~pH 2). This gave 4a (0.888 g, 81%) as a brown powder. Mp 279.0–280.0 °C; ν_{max}/cm^{−1} 3290m (N–H), 3078m (C–H), 1644s (C=O), 1560s, 1534s, 1508s; δ_H (500 MHz, DMSO-*d*₆) 11.91 (1H, s br, NH), 10.74 (1H, s br, NH), 10.33 (3H, s br, NH₃), 7.80 (1H, d, J 9.2, C(5)H), 7.59 (1H, d, J 8.9, C(3)H), 7.56 (1H, d, J 2.9, C(8)H), 7.43 (1H, dd, J 9.2, 2.9, C(6)H), 6.45 (1H, d, J 8.9, C(2)H), 3.84 (3H, s, OCH₃), 3.73 (2H, t, J 6.7, C(11)H₂), 3.32 (2H, t, J 6.7, C(12)H₂), 2.83 (6H, s, C(13)H₃, C(14)H₃); δ_C (75 MHz, DMSO-*d*₆) 178.8 (q), 154.6 (q), 150.5 (q), 136.4 (q), 134.7 (q), 129.8 (C(3)H), 124.1 (C(6)H), 121.4 (q), 118.8 (C(5)H), 106.5 (q), 105.4 (q), 104.8 (C(8)H), 98.7 (C(2)H), 55.4 (OCH₃), 54.3 (C(12)H₂), 42.4 (C(13)H₃, C(14)H₃), 37.3 (C(11)H₂); *m/z* (+ES) 327 (100, [M + H]⁺); 327.1819 ([M + H]⁺) found by +ES, required 327.1816, error 1.1 ppm.

Synthesis of 4-Amino-1-(2-(dimethylamino)ethylamino)-7-fluoroacridin-9(10*H*)-one Hydrochloride (4b). Raney Ni (750 mg) was added to a suspension of 3b (1.03 g, 3.00 mmol) and hydrazine monohydrate (0.6 mL) in THF (15 mL), and the reaction mixture was stirred for 1 h. The solution was filtered through Celite, washed with THF (2.0 mL), and the filtrate was adjusted with concentrated HCl to pH 3 and stirred for 30 min. The resulting brown precipitate was collected by filtration and recrystallized from MeOH–dioxane (9:1) (acidified with HCl to ~pH 2). This gave 4b (0.968 g, 91%) as a green powder. Mp 259.0–260.0 °C; ν_{max}/cm^{−1} 3439m (N–H), 3192m, 2966m (C–H), 1647s (C=O); δ_H (500 MHz, DMSO-*d*₆) 12.08 (1H, s br, NH), 10.69 (1H, s br, NH), 10.18 (3H, s br, NH₃), 7.92 (1H, dd, J 8.8, 4.4, C(5)H), 7.80 (1H, dd, J 8.8, 2.2, C(8)H), 7.68 (1H, app dt, J 8.8, 2.2, C(6)H), 7.62 (1H, d, J 8.8, C(3)H), 6.51 (1H, d, J 8.8, C(2)H), 3.74 (2H, t, J 6.5, C(11)H₂), 3.31 (2H, t, J 6.5, C(12)H₂), 2.82 (6H, s, C(13)H₃, C(14)H₃); δ_C (125 MHz, DMSO-*d*₆) 178.7 (q), 158.5 (d, J 236.6, C(7)F), 150.6 (q), 136.8 (q), 136.5 (q), 130.6 (C(3)H), 122.6 (d, J 24.5, C(6)H), 121.5 (d, J 6.3, q), 119.6 (d, J 8.2, C(5)H), 109.5 (d, J 22.7, C(8)H), 106.5 (q), 105.4 (q), 99.5 (C(2)H), 54.2 (C(12)H₂), 42.5 (C(13)H₃, C(14)H₃), 37.3 (C(11)H₂); δ_F (376 MHz, CDCl₃) −118.91, −117.94 (m); *m/z* (+ES) 315 (100, [M + H]⁺); 315.1603 ([M + H]⁺) found by +ES, required 315.1616, error 4.0 ppm.

Synthesis of 4-Amino-1-(2-(dimethylamino)ethylamino)-acridin-9(10*H*)-one Hydrochloride (4c). Raney Ni (750 mg) was added to a suspension of 3c (0.980 g, 3.00 mmol) and hydrazine monohydrate (0.6 mL) in THF (15 mL), and the reaction mixture was stirred for 1 h. The resulting solution was filtered through Celite, washed with THF (2.0 mL), and the filtrate was adjusted with concentrated HCl to pH 3 and stirred for 30 min. The resulting brown precipitate was collected by filtration and purified by recrystallization from MeOH–dioxane (9:1) (acidified with HCl to ~pH 2). This gave 4c (0.991 g, 99%) as a brown powder. Mp 249.0–251.0 °C; ν_{max}/cm^{−1} 3396m (N–H), 3064m (C–H), 1640s (C=O), 1611s, 1599s; δ_H (500 MHz, DMSO-*d*₆) 11.86 (1H, s br, NH), 10.28 (1H, s br, NH), 10.00 (3H, s br, NH₃),

8.17 (1H, d, J 7.8, C(8)H), 7.82 (1H, d, J 7.8, C(5)H), 7.73 (1H, app t, J 7.8, C(6)H), 7.61 (1H, d, J 8.8, C(3)H), 7.29 (1H, app t, J 7.8, C(7)H), 6.51 (1H, d, J 8.8, C(2)H), 3.74 (2H, t, J 6.5, C(11)H₂), 3.32 (2H, t, J 6.5, C(12)H₂), 2.82 ((6H, s, C(13)H₃, C(14)H₃); δ_C (75 MHz, DMSO-*d*₆) 179.5 (q), 150.6 (q), 140.0 (q), 136.8 (q), 133.7 (C(4)H), 130.2 (C(3)H), 125.5 (C(8)H), 122.0 (C(7)H), 120.8 (q), 117.0 (C(5)H), 106.9 (q), 105.5 (q), 99.4 (C(2)H), 54.3 (C(12)H₂), 42.4 (C(13)H₃, C(14)H₃), 37.2 (C(11)H₂); *m/z* (+ES) 297 (100, [M + H]⁺); 297.1706 ([M + H]⁺) found by +ES, required 297.1710, error 1.3 ppm.

Synthesis of 1-(2-(Dimethylamino)ethylamino)-4-amino-7-bromoacridin-9(10*H*)-one Hydrochloride (4d). Raney Ni (285 mg) was added to a suspension of 3d (0.770 g, 1.90 mmol) and hydrazine monohydrate (0.34 mL) in THF (20 mL), and the reaction mixture was stirred for 1 h. The resulting solution was filtered through Celite, washed with THF (2.0 mL), and the filtrate was adjusted with concentrated HCl to pH 3 and stirred for 30 min. The resulting brown precipitate was collected by filtration and purified by recrystallization from MeOH–dioxane (9:1) (acidified with HCl to ~pH 2). This gave 4d (0.630 g, 88%) as a green powder. ν_{max}/cm^{−1} 3301m (N–H), 3077m, 3024m, 2998sm, 2956m (C–H), 1649s (C=O), 1614m, 1598s, 1562s, 1548s, 1508s; δ_H (300 MHz, DMSO-*d*₆) 12.09 (1H, s, NH), 10.64 (1H, s br, NH), 10.13 (3H, s br, NH₃), 8.21 (1H, s, C(8)H), 7.89–7.80 (2H, m, C(5)H, C(6)H), 7.62 (1H, d, J 8.9, C(3)H), 6.53 (1H, d, J 8.9, C(2)H), 3.74 (2H, t, J 6.5, C(12)H₂), 3.31 (2H, t, J 6.5, C(11)H₂), 2.83 (6H, s, C(13)H₃, C(14)H₃); δ_C (75 MHz, DMSO-*d*₆) 178.2 (q), 150.5 (q), 138.9 (q), 136.5 (C(6)H), 136.2 (q), 130.4 (C(3)H), 127.4 (C(8)H), 122.1 (q), 119.5 (C(5)H), 114.0 (q), 106.9 (q), 105.8 (q), 99.9 (C(2)H), 54.2 (C(11)H₂), 42.4 (C(13)H₃, C(14)H₃), 37.2 (C(12)H₂); (+ES) 377 (100, [M + H]⁺, ⁸¹Br), 375 (100, [M + H]⁺, ⁷⁹Br); 375.0805 ([M + H]⁺) found by +ES, required 375.0815, error 2.7 ppm.

Synthesis of 4-Amino-1-(2-(dimethylamino)ethylamino)-7-hydroxyacridin-9(10*H*)-one Hydrochloride (4e). Raney Ni (750 mg) was added to a suspension of 3e (1.07 g, 3.00 mmol) and hydrazine monohydrate (0.6 mL) in THF (15 mL), and the reaction mixture was stirred for 24 h. The resulting solution was filtered through Celite, washed with THF (20 mL), and the filtrate was adjusted with concentrated HCl to pH 3 and stirred for 30 min. The resulting brown precipitate was collected by filtration and purified by recrystallization from MeOH–dioxane (9:1) (acidified with HCl to ~pH 2). This gave 4e (0.751 g, 72%) as a brown powder. Mp 230.8–231.4 °C; ν_{max}/cm^{−1} 3323m (N–H), 3025m, 2958m, 2819 (C–H), 1655s (C=O); δ_H (500 MHz, DMSO-*d*₆) 11.49 (1H, s, NH), 10.54 (1H, s, OH), 10.34 (1H, s br, NH), 10.21 (3H, s br, NH₃), 9.73 (1H, s br, NH), 7.68 (1H, d, J 8.8, C(5)H), 7.52–7.30 (2H, m, C(3)H, C(8)H), 7.29 (1H, dd, J 8.8, 2.8, C(6)H), 6.39 (1H, d, J 8.8, C(2)H), 3.70 (2H, s br, C(11)H₂), 3.33 (2H, s br, C(12)H₂), 2.84 (6H, s, C(13)H₃, C(14)H₃); *m/z* (+ES) 313 (100, [M + H]⁺); 313.1648 ([M + H]⁺) found by +ES, required 313.1659, error 3.1 ppm.

Synthesis of 4-Amino-1-(2-(diethylamino)ethylamino)-7-hydroxyacridin-9(10*H*)-one Hydrochloride (4f). Raney Ni (750 mg) was added to a suspension of 3f (1.07 g, 3.00 mmol) and hydrazine monohydrate (0.6 mL) in THF (15 mL), and the reaction mixture was stirred for 24 h. The solution was filtered through Celite, washed with THF (2.0 mL), and the filtrate was adjusted with concentrated HCl to pH 3 and stirred for 30 min. The resulting brown precipitate was collected by filtration and purified by recrystallization from MeOH–dioxane (9:1) (acidified with HCl to ~pH 2). This gave 4f (0.645 g, 57%) as a brown powder. Mp 337.5–339.5 °C; ν_{max}/cm^{−1} 3385m (O–H), 3212m (N–H), 2967m (C–H), 1667s (C=O), 1641s, 1584s; δ_H (300 MHz, DMSO-*d*₆) 11.26 (1H, s, NH), 10.97 (1H, s, OH), 10.31 (1H, s br, NH), 7.81 (1H, d, J 8.9, C(5)H), 7.51 (1H, d, J 2.0, C(8)H), 7.22 (1H, m, C(6)H), 7.06 (1H, d, J 8.2, C(3)H), 6.35 (1H, d, J 8.2, C(2)H), 4.10

(3H, s br, NH₃), 3.64 (2H, t, J 6.4, C(11)H₂), 3.32 (2 H, t, J 6.4, C(12)H₂), 3.19 (4H, q, J 7.0, C(13)H₂), 1.23 (6H, t, J 7.0, 2 × CH₃); δ_C (75 MHz, DMSO-*d*₆) 178.9 (q), 158.5 (q), 152.1 (q), 133.9 (q), 132.7 (q), 123.8 (C(6)H), 121.8 (q), 119.3 (C(5)H), 117.3 (C(3)H), 108.0 (C(8)H), 107.6 (q), 102.9 (C(2)H), 102.7 (q), 48.8 (C(12)H₂), 46.8 (CH₂), 30.7 (C(11)H₂), 8.5 (CH₃); *m/z* (−ES) 339 (100, [M − H][−]); (+ES) 341 (100, [M + H]⁺); 341.1982 ([M + H]⁺) found by +ES, required 341.1973, error 2.8 ppm.

Synthesis of 5-(2-(Dimethylamino)ethylamino)-8-methoxy-6H-imidazo[4,5,1-*de*]acridin-6-one (5a1). 4a (182 mg, 0.50 mmol) was heated under reflux in trimethyl orthoformate (2.0 mL) for 24 h. The solvent was removed under vacuum and the solid residue was purified by recrystallization from ethanol to give 5a1 (150 mg, 89%). Mp 219.0–219.4 °C; ν_{max}/cm^{−1} 3264m (N–H), 3076m (C–H), 1656s (C=O), 1601, 1577s, 1535s; δ_H (300 MHz, CDCl₃) 9.12 (1H, s br, NH), 8.51 (1H, s, C(1)H), 8.01–7.97 (2H, m, C(3)H, C(7)H), 7.86 (1H, d, J 8.9, C(10)H), 7.38 (1H, dd, J 8.9, 3.0, C(9)H), 6.76 (1H, d, J 9.0, C(4)H), 3.97 (2H, s, OCH₃), 3.53 (2H, app q, J 6.0, C(12)H₂), 2.74 (2H, t, J 6.4, C(13)H₂), 2.40 (6H, s, C(14)H₃, C(15)H₃); δ_C (75 MHz, CDCl₃) 178.2 (q), 157.3 (q), 150.2 (q), 133.0 (C(1)H), 132.7 (q), 131.0 (q), 129.4 (C(3)H), 129.3 (q), 126.9 (q), 122.5 (C(9)H), 116.1 (C(10)H), 109.0 (C(7)H), 106.6 (C(4)H), 102.9 (q), 77.4 (q), 77.0 (q), 76.6 (q), 57.9 (C(13)H₂), 55.9 (OCH₃), 45.5 (C(14)H₃, C(15)H₃), 41.0 (C(12)H₂); *m/z* (+ES) 359 (40, [M + Na]⁺), 337 (100, [M + H]⁺); 337.1650 ([M + H]⁺) found by +ES, required 337.1659, error 2.7 ppm.

Synthesis of 5-(2-(Dimethylamino)ethylamino)-8-fluoro-6H-imidazo[4,5,1-*de*]acridin-6-one (5b1). 4b (176 mg, 0.50 mmol) was heated under reflux in trimethyl orthoformate (2.0 mL) for 24 h. The solvent was removed under vacuum and the residue was purified by recrystallization from ethanol to give 5b1 (150 mg, 68%). Mp 190.6–191.8 °C; ν_{max}/cm^{−1} 3275m (N–H), 3074m, 2976m (C–H), 1657s (C=O), 1605s, 1576s; δ_H (300 MHz, DMSO-*d*₆) 9.20 (1H, s, C(1)H), 8.94 (1H, t, J 4.6, NH), 8.51 (1H, dd, J 8.9, 4.5, C(10)H), 8.04 (1H, dd, J 9.1, 3.0, C(7)H), 8.01 (1H, d, J 9.1, C(3)H), 7.86 (1H, app dt, J 8.9, 3.0, C(9)H), 6.83 (1H, d, 9.1, C(4)H), 3.45 (2H, app q, J 5.6, C(12)H₂), 2.60 (2H, t, J 6.1, C(13)H₂), 2.25 (6H, s, C(14)H₃, C(15)H₃); *m/z* (+ES) 347 (40, [M + Na]⁺), 325 (100, [M + H]⁺); 325.1459 ([M + H]⁺) found by +ES, required 325.1459, error 0.0 ppm.

Synthesis of 5-(2-(Dimethylamino)ethylamino)-6H-imidazo[4,5,1-*de*]acridin-6-one (5c1). 4c (167 mg, 0.50 mmol) was heated under reflux in trimethyl orthoformate (2.0 mL) for 24 h. The solvent was removed under vacuum and the residue was purified by recrystallization from ethanol to give 5c1 (89 mg, 51%). Mp 215.8–216.6 °C; ν_{max}/cm^{−1} 3282m (N–H), 3077m, 2971m, 2937m, 2863m, 2815, (C–H), 1660s (C=O), 1622, 1598s; δ_H (300 MHz, DMSO-*d*₆) 9.23 (1H, s, C(1)H), 8.98 (1H, t, J 4.5, NH), 8.38–8.44 (2H, m, C(7)H, C(10)H), 8.01 (1H, d, J 8.9, C(3)H), 7.93 (1H, app t, J 7.7), 7.60 (1H, app t, J 7.6), 6.84 (1H, d, J 8.9, C(4)H), 3.46 (2H, app q, J 5.6, C(12)H₂), 2.60 (2H, t, J 6.1, C(13)H₂), 2.25 (6H, s, C(14)H₃, C(15)H₃); δ_C (125 MHz, DMSO-*d*₆) 177.6 (q), 149.3 (C(1)H), 135.5 (q), 134.9 (q), 133.8 (CH), 132.5 (q), 130.6 (q), 129.2 (CH), 127.4 (C(7)H), 125.5 (CH), 124.9 (q), 116.3 (C(10)H), 107.0 (C(4)H), 102.4 (q), 57.4 (C(13)H₂), 45.2 (C(14)H₃, C(15)H₃), 40.2 (C(12)H₂); *m/z* (+ES) 329 (95, [M + Na]⁺), 307 (100, [M + H]⁺); 307.1547 ([M + H]⁺) found by +ES, required 307.1553, error 2.1 ppm.

Synthesis of 5-(2-(Dimethylamino)ethylamino)-8-hydroxy-6H-imidazo[4,5,1-*de*]acridin-6-one (5e1). 4e (175 mg, 0.50 mmol) was heated under reflux in trimethyl orthoformate (2.0 mL) for 24 h. The solvent was removed under vacuum and the residue was purified by recrystallization from ethanol to give 5e1 (155 mg, 96%). Mp 291.0–292.0 °C; ν_{max}/cm^{−1} 3354br (O–H), 3173m (N–H), 3072m, 2969m (C–H), 1668s (C=O), 1631s, 1586s, 1561s, 1530s; δ_H (300 MHz, DMSO-*d*₆) 10.13 (1H, s br, OH), 9.12 (1H, s, C(1)H), 8.97 (1H, t, J 4.9, NH), 8.28 (1H, d, J 9.0, C(10)H), 7.99 (1H, d, J 8.8, C(3)H), 7.72 (1H, d, J 2.9, C(7)H), 7.34 (1H, dd, J 9.0, 2.9, C(9)H), 6.82 (1H, d,

J 8.8, C(4)H), 3.45 (2H, app q, J 5.6, C(12)H₂), 2.60 (2H, t, J 6.2, C(13)H₂), 2.25 (6H, s, C(14)H₃, C(15)H₃); δ_C (75 MHz, DMSO-*d*₆) 177.6 (q), 155.8 (q), 148.8 (q), 142.1 (q), 135.4 (C(1)H), 127.8 (q), 127.5 (q), 126.2 (q), 122.4 (C(9)H), 120.7 (C(3)H), 117.9 (C(10)H), 111.3 (C(7)H), 107.6 (C(4)H), 102.2 (q), 54.6 (C(12)H₂), 42.4 (C(13)H₂), 30.7 (C(14)H₃, C(15)H₃); *m/z* (−ES) 321 (100, [M − H][−]); (+ES) 345 (20, [M + Na]⁺), 323 (100, [M + H]⁺); 323.1507 ([M + H]⁺) found by +ES, required 323.1503, error 1.4 ppm.

Synthesis of 5-(2-(Diethylamino)ethylamino)-8-hydroxy-6H-imidazo[4,5,1-*de*]acridin-6-one (5f1). 4f (189 mg, 0.50 mmol) was heated under reflux in trimethyl orthoformate (2.0 mL) for 24 h. The solvent was removed under vacuum and the residue was purified by recrystallization from ethanol to give 5f1 (80 mg, 46%). Mp 272.0–274.0 °C; ν_{max}/cm^{−1} 3375br (O–H), 3275m (N–H), 3041m, 2951 (C–H), 1667s (C=O), 1587s, 1566s, 1530s; δ_H (300 MHz, DMSO-*d*₆) 10.16 (1H, s br), 10.06 (1H, s br), 9.27 (1H, s, C(1)H), 8.95 (1H, s br, NH), 8.31 (1H, d, J 8.7, C(10)H), 8.05 (1H, d, J 8.8, C(3)H), 7.75 (1H, d, J 2.8, C(7)H), 7.38 (1H, dd, J 8.9, 2.8, C(9)H), 7.02 (1H, d, J 8.9, C(4)H), 3.90 (2H, s br, C(12)H₂), 3.35 (2H, app q, C(13)H₂), 3.23 (4H, s br, C(14)H₂, C(16)H₂), 1.23 (6H, t, J 7.2, C(15)H₂, C(17)H₂); δ_C (75 MHz, DMSO-*d*₆) 177.3 (q), 163.0 (q), 157.5 (q), 156.1 (q), 149.0 (q), 135.0 (C(1)H), 127.1 (q), 126.3 (q), 122.3 (C(9)H), 120.9 (C(3)H), 118.1 (C(10)H), 111.4 (C(7)H), 108.4 (C(4)H), 101.8 (q), 49.0 (C(13)H₂), 46.5 (C(14)H₂, C(16)H₂), 37.3 (C(12)H₂), 8.3 (CH₃); *m/z* (−ES) 349 (100, [M − H][−]); (+ES) 351 (30, [M + H]⁺); 351.1807 ([M + H]⁺) found by +ES, required 351.1816, error 2.6 ppm.

Synthesis of 5-(2-(Dimethylamino)ethylamino)-8-methoxy-6H-imidazo[4,5,1-*de*]acridin-6-one *N*-Oxide (6a1). *m*-CPBA (69.2 mg, 0.2 mmol) was added to a suspension of 5a1 (33.6 mg, 0.10 mmol) in CHCl₃ (3.0 mL), and the reaction mixture was stirred for 18 h at room temperature. The mixture was then passed through a column of alumina, eluting sequentially with CHCl₃ (400 mL) followed by CHCl₃/MeOH (9:1, 400 mL) to remove 5a1 and finally by CHCl₃/MeOH (3:1, 500 mL) to elute the target compound. The final fraction was concentrated in vacuo to give 6a1 (32.0 mg, 91%). Mp 112.6–113.6 °C; ν_{max}/cm^{−1} 3245m (N–H), 3089m, 2957m (C–H), 1654s (C=O), 1574s, 1532s; δ_H (500 MHz, DMSO-*d*₆) 9.59 (1H, s br, NH), 9.15 (1H, s, C(1)H), 8.36 (1H, d, J 8.5, C(10)H), 7.98 (1H, d, J 8.5, C(2)H), 7.76 (1H, s, C(7)H), 7.53 (1H, d, J 8.5, C(9)H), 6.93 (1H, d, J 8.5, C(3)H), 3.94–3.92 (5H, m, CH₃, C(13)H₂), 3.55 (2H, s br, C(12)H₂), 3.15 (6H, s, 2 × CH₃); *m/z* (+ES) 375 (100, [M + Na]⁺), 353 (10, [M + H]⁺); 375.1437 ([M + Na]⁺) found by +ES, required 375.1428, error 2.5 ppm.

Synthesis of 5-(2-(Dimethylamino)ethylamino)-8-fluoro-6H-imidazo[4,5,1-*de*]acridin-6-one *N*-Oxide (6b1). *m*-CPBA (69.2 mg, 0.2 mmol) was added to a suspension of 5b1 (32.4 mg, 0.10 mmol) in CHCl₃ (3.0 mL), and the reaction mixture was stirred at room temperature for 18 h. The mixture was then passed through a column of alumina, eluting sequentially with CHCl₃ (400 mL), CHCl₃/MeOH (9:1, 400 mL) to remove 5b1, and finally CHCl₃/MeOH (3:1, 500 mL) to elute the target compound. The final fraction was concentrated in vacuo to give 6b1 (29.0 mg, 85%). Mp 116–118 °C; ν_{max}/cm^{−1} 3237m (N–H), 3095m (C–H), 1652s (C=O), 1575s, 1527s; δ_H (300 MHz, DMSO-*d*₆) 9.49 (1H, J 5.5, NH), 9.22 (1H, s, C(1)H), 8.53 (1H, dd, J 8.8, 3.7, C(10)H), 8.03 (2H, m, C(3)H, C(7)H), 7.88 (1H, app dt, J 8.8, 3.0, C(9)H), 6.99 (1H, d, J 9.0, C(4)H), 3.93 (2H, app q, J 5.6, C(12)H₂), 3.54 (2H, t, J 6.0, C(13)H₂), 3.12 (6H, s, C(14)H₂, C(15)H₂); *m/z* (+ES) 363 (100, [M + Na]⁺), 341 (40, [M + H]⁺); 363.1232 ([M + Na]⁺) found by +ES, required 363.1228, error 1.2 ppm.

Synthesis of 5-(2-(Dimethylamino)ethylamino)-6H-imidazo[4,5,1-*de*]acridin-6-one *N*-Oxide (6c1). *m*-CPBA (69.2 mg, 0.2 mmol) was added to a suspension of 5c1 (30.6 mg, 0.10 mmol) in CHCl₃ (3.0 mL), and the reaction mixture was stirred at room temperature for 18 h. The mixture was then passed through a column of alumina, eluting

sequentially with CHCl_3 (400 mL), $\text{CHCl}_3/\text{MeOH}$ (9:1, 400 mL) to remove **5c1**, and finally $\text{CHCl}_3/\text{MeOH}$ (3:1, 500 mL) to elute the target compound. The final fraction was concentrated in vacuo to give **6c1** (30 mg, 93%). Mp 110.5–111.5 °C; $\nu_{\text{max}}/\text{cm}^{-1}$ 3242m (N–H), 3072m, 2959m (C–H), 1646s (C=O), 1579s; δ_{H} (300 MHz, $\text{DMSO}-d_6$) 9.60 (1H, s br, NH), 9.25 (1H, s, C(1)H), 8.19 (1H, d, J 8.5, C(10)H), 7.97 (1H, d, J 8.4, C(2)H), 7.85 (1H, s, C(7)H), 7.63 (1H, app t, J 8.3, C(9)H), 7.54 (1H, app t, J 8.3, C(8)H), 6.93 (1H, d, J 8.4, C(3)H), 3.90–3.86 (5H, m, CH_3 , C(13)H₂), 3.55 (2H, s br, C(12)H₂), 3.15 (6H, s, 2 × CH₃); m/z 321 (40, [M – H][–]); (+ES) 345 (100, [M + Na]⁺), 323 (100, [M + H]⁺); 345.1322 ([M + Na]⁺) found by +ES, required 345.1322, error 0.0 ppm.

Synthesis of 5-(2-(Dimethylamino)ethylamino)-8-hydroxy-6H-imidazo[4,5,1-de]acridin-6-one N-Oxide (6e1). *m*-CPBA (35.0 mg, 0.1 mmol) was added to a suspension of **5e1** (16.1 mg, 0.05 mmol) in CHCl_3 (2.0 mL), and the reaction mixture was stirred at room temperature for 18 h. The mixture was then passed through a column of alumina, eluting sequentially with CHCl_3 (400 mL), $\text{CHCl}_3/\text{MeOH}$ (9:1, 400 mL) to remove **5e1**, and finally $\text{CHCl}_3/\text{MeOH}$ (3:1, 1.0 L) to elute the target compound. The final fraction was concentrated in vacuo to give a pale yellow powder that was dissolved in MeOH (3 mL) and filtered to remove residual silica. The solvent was removed to give **6e1** (5.0 mg, 30%). δ_{H} (500 MHz, $\text{DMSO}-d_6$) 10.56 (1H, s br, OH), 9.35 (1H, s br, NH), 9.00 (1H, s, C(1)H), 8.14 (1H, d, J 8.7, C(3)H), 7.81 (1H, d, J 8.9, C(10)H), 7.65 (1H, d, J 2.5, C(7)H), 7.28 (1H, dd, J 8.9, 2.5, C(9)H), 6.76 (1H, d, J 8.7, C(4)H), 3.89 (2H, app q, J 5.6, C(12)H₂), 3.73 (2H, s br, C(13)H₂), 3.26 (6H, s, C(14)H₃, C(15)H₃); m/z (–ES) 337 (70, [M – H][–]); 337.1302 ([M – H][–]) found by –ES, required 337.1301, error 0.1 ppm.

Synthesis of 5-(2-(Dimethylamino)ethylamino)-8-methoxy-1-methyl-6H-imidazo[4,5,1-de]acridin-6-one (5a2). **4a** (182 mg, 0.50 mmol) was heated under reflux in trimethyl orthoacetate (2.0 mL) for 24 h. The solvent was removed under vacuum and the residue was purified by recrystallization from ethanol to give **5a2** (170 mg, 97%). Mp 205.0–206.0 °C; $\nu_{\text{max}}/\text{cm}^{-1}$ 3270w (N–H), 3002w, 2975w, 2946w, 2885w, 2848m, 2811m, 2760m (C–H), 1756s (C=O), 1652s, 1608s; δ_{H} (300 MHz, CDCl_3) 9.14 (1H, s br, NH), 8.09 (1H, d, J 3.0, C(7)H), 8.04 (1H, d, J 9.1, C(10)H), 7.89 (1H, d, J 8.8, C(3)H), 7.38 (1H, dd, J 9.1, 3.0, C(9)H), 6.71 (1H, d, J 8.8, C(4)H), 3.99 (3H, s, OC(17)H₃), 3.55 (2H, app q, C(13)H₂), 3.12 (3H, s br, C(11)H₃), 2.78 (2H, t, C(14)H₂), 2.42 (6H, s, C(15)H₃, C(16)H₃); δ_{C} (75 MHz, CDCl_3) 178.2 (q), 156.7 (q), 149.5 (q), 145.8 (q), 134.5 (q), 130.9 (q), 129.4 (q), 128.1 (C(3)H), 127.6 (q), 122.0 (C(9)H), 117.3 (C(10)H), 109.4 (C(7)H), 105.6 (C(4)H), 103.1 (q), 58.0 (C(14)H₂), 55.8 (OC(17)H₃), 45.6 (C(15)H₃, C(16)H₃), 41.0 (C(13)H₂), 19.0 (C(11)H₃); m/z (+ES) 373 (40, [M + Na]⁺), 351 (100, [M + H]⁺); 351.1811 ([M + H]⁺) found by +ES, required 351.1816, error 1.3 ppm.

Synthesis of 5-(2-(Dimethylamino)ethylamino)-8-fluoro-1-methyl-6H-imidazo[4,5,1-de]acridin-6-one (5b2). **4b** (176 mg, 0.50 mmol) was heated under reflux in trimethyl orthoacetate (2.0 mL) for 24 h. The solvent was removed under vacuum and the residue was purified by recrystallization from ethanol to give **5b2** (150 mg, 89%). Mp 189.2–198.0 °C; $\nu_{\text{max}}/\text{cm}^{-1}$ 3265m (N–H), 3037m, 2968m, 2935m (C–H), 1652s (C=O), 1604s, 1581s, 1540s, 1525s; δ_{H} (300 MHz, CDCl_3) 9.09 (1H, s br, NH), 8.31 (1H, dd, J 9.0, 3.2, C(7)H), 8.11 (1H, dd, J 9.3, 4.3, C(10)H), 7.91 (1H, d, J 8.9, C(3)H), 7.53 (1H, app dt, J 8.1 3.2, C(9)H), 6.76 (1H, d, J 8.9, C(4)H), 3.62 (2H, s br, C(13)H₂), 3.13 (3H, s, C(11)H₃), 2.84 (2H, s br, C(14)H₂), 2.48 (6H, s, C(15)H₃, C(16)H₃); m/z (+ES) 361 (20, [M + Na]⁺), 339 (100, [M + Na]⁺); 339.1616 ([M + H]⁺) found by +ES, required 339.1616, error 0.1 ppm.

Synthesis of 5-(2-(Dimethylamino)ethylamino)-1-methyl-6H-imidazo[4,5,1-de]acridin-6-one (5c2). **4c** (182 mg, 0.50 mmol) was heated under reflux in trimethyl orthoacetate (2.0 mL) for 24 h. The solvent was removed under vacuum and the residue was purified by recrystallization from ethanol to give **5c2** (48 mg, 28%). Mp 258.0–260.0 °C; $\nu_{\text{max}}/\text{cm}^{-1}$

3314m (N–H), 2990m, 2964m, 2905m (C–H), 1652s (C=O), 1602s, 1582s, 1569s; δ_{H} (300 MHz, $\text{DMSO}-d_6$) 9.01 (1H, t, J 4.9, NH), 8.47 (1H, dd, J 7.9 1.7, C(7)H), 8.27 (1H, d, J 8.5, C(10)H), 7.92 (1H, app dt, 7.8, 1.7, C(9)H), 7.88 (1H, d, J 8.8, C(3)H), 7.60 (1H, app t, J 7.6, C(8)H), 6.77 (1H, d, J 8.8, C(4)H), 3.43 (2H, app q, J 5.7, C(13)H₂), 3.08 (3H, s, C(11)H₃), 2.60 (2H, t, J 6.0, C(14)H₂), 2.25 (6H, s, C(15)H₃, C(16)H₃); δ_{C} (75 MHz, $\text{DMSO}-d_6$) 177.6 (q), 148.2 (q), 147.0 (q), 136.1 (C(9)H), 133.8 (C(10)H), 129.4 (q), 127.8 (q), 127.6 (q), 125.2 (C(8)H), 124.9 (q), 117.0 (C(7)H), 111.1 (C(3)H), 105.8 (C(4)H), 102.8 (q), 56.2 (C(14)H₂), 44.0 (C(15)H₃, C(16)H₃), 43.9 (C(13)H₂), 18.5 (C(11)H₃); m/z (+ES) 343 (50, [M + Na]⁺), 321 (100, [M + H]⁺); 343.1536 ([M + H]⁺) found by +ES, required 343.1529, error 1.9 ppm.

Synthesis of 5-(2-(Dimethylamino)ethylamino)-8-bromo-1-methyl-6H-imidazo[4,5,1-de]acridin-6-one (5d2). **4d** (94 mg, 0.25 mmol) was heated under reflux in trimethyl orthoacetate (2.0 mL) for 24 h. The solvent was removed under vacuum and the residue was purified by recrystallization from ethanol to give **5d2** (45 mg, 45%). Mp 176.0–177.0 °C; $\nu_{\text{max}}/\text{cm}^{-1}$ 3274m (N–H), 3113m, 3056w, 2968w (C–H), 1690s (C=O), 1651m, 1618s, 1596s; δ_{H} (300 MHz, CDCl_3) 9.09 (1H, s br, NH), 8.77 (1H, d, J 2.4, C(7)H), 7.99 (1H, d, J 8.9), 7.90–7.86 (2H, m), 6.73 (1H, d, J 8.7), 3.58 (2H, app q, J 5.3, C(13)H₂), 3.11 (3H, s, C(11)H₃), 2.80 (2H, t, J 5.4, C(14)H₂), 2.45 (6H, s, C(15)H₃, C(16)H₃); m/z (+ES) 423 (70, [M + Na]⁺, ⁸¹Br), 421 (70, [M + Na]⁺, ⁷⁹Br), 401 (100, [M + H]⁺, ⁸¹Br), 399 (100, [M + H]⁺, ⁷⁹Br); 399.0825 ([M + H]⁺) found by +ES, required 399.0815, error 2.5 ppm.

Synthesis of 5-(2-(Dimethylamino)ethylamino)-8-hydroxy-1-methyl-6H-imidazo[4,5,1-de]acridin-6-one (5e2). **4e** (182 mg, 0.50 mmol) was heated under reflux in trimethyl orthoacetate (2.0 mL) for 24 h. The solvent was removed under vacuum and the residue was purified by recrystallization from ethanol to give **5e2** (67 mg, 40%). Mp 295.5–298.0 °C; $\nu_{\text{max}}/\text{cm}^{-1}$ 3289m (N–H), 2967m, 2930m, 2861m (C–H), 1651s (C=O), 1604s, 1582s, 1536s, 1520s; δ_{H} (300 MHz, $\text{DMSO}-d_6$) 10.17 (1H, s br, NH), 10.01 (1H, s br, OH), 8.97 (1H, s br, NH), 8.16 (1H, d, J 9.2, C(10)H), 7.93 (1H, d, J 8.7, C(3)H), 7.82 (1H, d, J 2.9, C(7)H), 7.38 (1H, dd, J 9.2, 2.9, C(9)H), 6.92 (1H, d, J 8.7, C(4)H), 3.86 (2H, app q, J 6.5, C(12)H₂), 3.06 (3H, s, CH₃), 2.50 (observed, C(13)H₂), 2.87 (6H, d, J 4.3, 2 × CH₃); m/z (–ES) 335 (100, [M – H][–]); (+ES) 337 (20, [M + H]⁺); 337.1652 ([M + H]⁺) found by +ES, required 337.1660, error 2.2 ppm.

Synthesis of 5-(2-(Diethylamino)ethylamino)-8-hydroxy-1-methyl-6H-imidazo[4,5,1-de]acridin-6-one (5f2). **4f** (189 mg, 0.50 mmol) was heated under reflux in trimethyl orthoacetate (2.0 mL) for 24 h. The solvent was removed under vacuum and the residue was purified by recrystallization from ethanol to give **5f2** (96 mg, 52%). Mp 254–255 °C; $\nu_{\text{max}}/\text{cm}^{-1}$ 3290m (N–H), 2967m, 2929m, 2865m (C–H), 1651s (C=O), 1604s, 1582s, 1536s, 1520s; δ_{H} (500 MHz, $\text{DMSO}-d_6$) 10.02 (1H, s, NH), 9.04 (1H, s br, NH), 8.13 (1H, d, J 9.1, C(10)H), 7.85 (1H, d, J 8.6, C(3)H), 7.81 (1H, d, J 2.9, C(7)H), 7.34 (1H, dd, J 9.1, 2.9, C(9)H), 6.73 (1H, d, J 8.6, C(4)H), 3.40 (observed, C(13)H₂), 3.03 (3H, s, C(11)H₃), 2.74 (2H, t, J 6.0, C(14)H₂), 2.58 (4H, q, J 7.2, 2 × CH₂), 1.03 (6H, t, J 7.2, 2 × CH₃); δ_{C} (75 MHz, $\text{DMSO}-d_6$) 177.2 (q), 154.6 (q), 148.6 (q), 146.1 (q), 133.8 (q), 129.2 (q), 128.9 (q), 127.6 (C(3)H), 126.9 (q), 121.7 (C(9)H), 118.4 (C(10)H), 111.8 (C(7)H), 105.5 (C(4)H), 102.1 (q), 50.8 (C(14)H₂), 46.4 (CH₂), 40.5 (C(13)H₂), 18.3 (C(11)H₃), 11.8 (CH₃); m/z (–ES) 363 (100, [M – H][–]); (+ES) 365 (40, [M + H]⁺); 365.1973 ([M + H]⁺) found by +ES, required 365.1972, error 0.3 ppm.

Synthesis of 5-(2-(Dimethylamino)ethylamino)-8-methoxy-1-methyl-6H-imidazo[4,5,1-de]acridin-6-one N-Oxide (6a2). *m*-CPBA (69 mg, 0.2 mmol) was added to a suspension of **5a2** (35.0 mg, 0.10 mmol) in CHCl_3 (3.0 mL), and the reaction mixture was stirred at room temperature for 18 h. The mixture was then passed through a column of alumina, eluting sequentially with CHCl_3 (400 mL), $\text{CHCl}_3/\text{MeOH}$ (9:1, 400 mL) to remove **5a2**, and finally $\text{CHCl}_3/\text{MeOH}$

(3:1, 500 mL) to elute the target compound. The final fraction was concentrated in vacuo to give **6a2** (25.0 mg, 69%). Mp 117.6–120.0 °C; $\nu_{\max}/\text{cm}^{-1}$ 3245m (N–H), 3089m, 2957m (C–H), 1654s (C=O), 1574s, 1532s; δ_{H} (500 MHz, DMSO- d_6) 9.60 (1H, s br, NH), 8.36 (1H, d, J 8.5, C(10)H), 7.98 (1H, d, J 8.5, C(2)H), 7.76 (1H, s, C(7)H), 7.38 (1H, d, J 8.5, C(9)H), 6.93 (1H, d, J 8.5, C(3)H), 3.94–3.92 (5H, m, CH₂, C(13)H₂), 3.55 (2H, s br, C(12)H₂), 3.15 (6H, s, 2 × CH₃), 2.40 (3H, s, CH₃); m/z (–ES) 365 (60, [M – H][–]); (+ES) 389 (20, [M + Na]⁺), 367 (10, [M + H]⁺); 365.1610 ([M – H][–]) found by –ES, required 365.1608, error 0.2 ppm.

Synthesis of 5-(2-(Dimethylamino)ethylamino)-8-fluoro-1-methyl-6H-imidazo[4,5,1-de]acridin-6-one N-Oxide (6b2). *m*-CPBA (69.2 mg, 0.2 mmol) was added to a suspension of **5b2** (33.8 mg, 0.10 mmol) in CHCl₃ (3.0 mL), and the reaction mixture was stirred at room temperature for 18 h. The mixture was then passed through a column of alumina, eluting sequentially with CHCl₃ (400 mL), CHCl₃/MeOH (9:1, 400 mL) to remove **5b2**, and finally CHCl₃/MeOH (3:1, 500 mL) to elute the target compound. The final fraction was concentrated in vacuo to give **6b2** (33.0 mg, 93%). Mp 130.5–132.5 °C; $\nu_{\max}/\text{cm}^{-1}$ 3247m (N–H), 3095m, 2976m (C–H), 1651s (C=O); δ_{H} (300 MHz, DMSO- d_6) 9.49 (1H, J 5.5, NH), 8.53 (1H, dd, J 8.4, 3.7, C(10)H), 7.99 (2H, m, C(3)H, C(7)H), 7.78 (1H, app dt, J 8.4, 3.0, C(9)H), 6.99 (1H, d, J 9.0, C(4)H), 3.93 (2H, app q, J 5.6, C(12)H₂), 3.54 (2H, t, J 6.0, C(13)H₂), 3.12 (6H, s, C(14)H₂, C(15)H₂), 2.41 (3H, s, CH₃); m/z (+ES) 377 (60, [M + Na]⁺), 355 (55, [M + H]⁺); 377.1378 ([M + Na]⁺) found by +ES, required 377.1384, error 1.7 ppm.

Synthesis of 5-(2-(Dimethylamino)ethylamino)-1-methyl-6H-imidazo[4,5,1-de]acridin-6-one N-Oxide (6c2). *m*-CPBA (69.2 mg, 0.2 mmol) was added to a suspension of **5c2** (34.2 mg, 0.10 mmol) in CHCl₃ (3.0 mL), and the reaction mixture was stirred for 18 h. The mixture was then passed through a column of alumina, eluting sequentially with CHCl₃ (400 mL), CHCl₃/MeOH (9:1, 400 mL) to remove **5c2**, and finally CHCl₃/MeOH (3:1, 500 mL) to elute the target compound. The final fraction was concentrated in vacuo to give **6c2** (32.0 mg, 95%). Mp 125.0–127.8 °C; $\nu_{\max}/\text{cm}^{-1}$ 3199m (N–H), 3098m, 2960m (C–H), 1646s (C=O); δ_{H} (300 MHz, DMSO- d_6) 9.01 (1H, t, J 4.9, NH), 8.47 (1H, dd, J 7.9, 2.0, C(7)H), 8.27 (1H, d, J 8.5, C(10)H), 7.92 (1H, app dt, J 7.8, 2.0, C(9)H), 7.88 (1H, d, J 8.8, C(3)H), 7.60 (1H, app t, J 7.3, C(8)H), 6.77 (1H, d, J 8.8, C(4)H), 3.94–3.92 (5H, m, CH₂, C(13)H₂), 3.55 (2H, s br, C(12)H₂), 3.15 (6H, s, 2 × CH₃), 3.08 (3H, s, CH₃); m/z (+ES) 359 (100, [M + Na]⁺), 337 (90, [M + H]⁺); 337.1655 ([M + H]⁺) found by +ES, required 337.1660, error 1.3 ppm.

Synthesis of 5-(2-(Dimethylamino)ethylamino)-8-bromo-1-methyl-6H-imidazo[4,5,1-de]acridin-6-one N-Oxide (6d2). *m*-CPBA (35 mg, 0.1 mmol) was added to a suspension of **5d2** (22 mg, 0.055 mmol) in CHCl₃ (3.0 mL), and the reaction mixture was stirred for 18 h. The mixture was then passed through a column of alumina, eluting sequentially with CHCl₃ (400 mL), CHCl₃/MeOH (9:1, 400 mL) to remove **5d2**, and finally CHCl₃/MeOH (3:1, 500 mL) to elute the target compound. The final fraction was concentrated in vacuo to give **6d2** (16.0 mg, 70%). Mp 127.0–129.0 °C; $\nu_{\max}/\text{cm}^{-1}$ 3259m (N–H), 3039m, 2977m, (C–H), 1656s (C=O); δ_{H} (300 MHz, DMSO- d_6) 9.52 (1H, s br, NH), 8.43 (1H, s br, C(7)H), 8.19 (1H, d, J 9.0, C(10)H), 8.05 (1H, dd, J 9.0, 1.7, C(9)H), 7.87 (1H, d, J 8.3, C(3)H), 6.88 (1H, d, J 8.3, C(4)H), 3.89 (2H, app q, J 5.7, C(12)H₂), 3.52 (2H, s br, C(13)H₂), 3.13 (6H, s, C(14)H₂, C(15)H₂), 3.04 (3H, s, CH₃); m/z (+ES) 439 (100, [M + Na]⁺, ⁸¹Br), 437 (100, [M + Na]⁺, ⁷⁹Br); 415.0764 ([M + H]⁺) found by +ES, required 415.0765, error 0.1 ppm.

Molecular Modeling. For docking purposes, the crystallographic coordinates of human NQO2 (PDB code 1QR2, resolution 2 Å)²¹ was obtained from the Brookhaven database. Hydrogen atoms were added to the structure, which included the protein and FAD, allowing for

appropriate ionization at physiological pH. The protonated complex was then minimized within Sybyl 7.3 (Tripos Ltd., St. Louis, MO) while holding all heavy atoms stationary. Inspection of the active site showed a reasonable internal hydrogen bond network within the protein.

For preparation of ligand structures, fragments from Sybyl 7.3 were used to construct the compounds. Ligands were subject to 1000 iterations of energy minimization using the steepest descent algorithm by means of the Tripos force field. For computational docking, the GOLD 4.1 software was used in combination with the ChemScore scoring function. GOLD uses a genetic algorithm (GA), whereby the molecular features of a protein–ligand complex are encoded as a chromosome. Since GOLD's internal definition of "lipophilic atoms" are nonaccepting sulfurs, nonpolar carbon atoms, and nonionic Cl, Br, or I, adoption of the default setup seemed likely to underestimate the aromatic/lipophilic nature of the receptor in the immediate vicinity of the isoalloxazine fragment of FAD, consequently causing a systematically low prediction of binding affinities for known active aromatic ligands. To avoid this probability, we re-atom-typed the FAD fragment as previously described.²³

The active site was defined as being any volume within 15 Å of N5 of the FAD cofactor. Each GA run comprised 100 000 genetic operations on an initial population of 100 members divided into five subpopulations. Operator weights for crossover, mutation, and migration were set to 95, 95, and 10, respectively. GOLD allows a user-definable number of GA runs per ligand, each of which starts from a different orientation. For these experiments, the number of GA runs was set to 10, and scoring of the docked poses was performed with the ChemScore scoring function. The top 10 solutions for each ligand were retained and analyzed for favorable interactions within the active site of NQO2, including low protein–ligand clash, ligand distortion energies, lipophilic contacts, and hydrogen bonding interactions.

The **5a1** crystal structure was prepared as described above for 1QR2. The active site for the crystal complex was defined as being any volume within 15 Å of the **5a1** crystal ligand. The ligands were docked using the same parameters as for the preceding experiments. The top 25 poses for each ligand were retained and compared to the **5a1** crystal ligand. In addition, each solution was analyzed within the active site of the enzyme as previously discussed.

Protein Expression and Purification. The overexpression of NQO2 was performed in BL21 codon+ cells induced with 1 mM isopropyl β -D-1-thiogalactopyranoside (IPTG) overnight at 20 °C. The protein was purified to homogeneity by HisTrap HP Ni²⁺ affinity chromatography followed by size exclusion chromatography on a Superdex S200 10/300 GL column. Samples were concentrated to 15 mg/mL and supplemented with 5 μ M FAD prior to crystallization experiments.

Crystallization, Refinement, and Model Building. Crystals of NQO2 ligand complex were achieved by cocrystallization in the presence of both **5a1** and **6a1**. Conditions were identified using the PACT premier matrix screen (Molecular Dimensions) on a Mosquito nanodrop crystallization robot. Crystals suitable for diffraction experiments were obtained by sitting drop vapor diffusion in 4 μ L drops containing equal volumes of protein and a solution containing 0.2 M sodium formate and 20% polyethylene glycol 3350. Data were collected on beamline I04 at the Diamond Light Source Facility and reduced and scaled with the X-ray Detector Software suite (XDS).²⁴

The NQO2–**5a1** and NQO2–**6a1** crystal structures were determined by molecular replacement using PHASER from PHENIX²⁵ and the human NQO2 structure (1QR2)²¹ as a starting model. Structures were completed by iterative cycles of manual model building and real space refinement using the program Coot²⁶ and crystallographic refinement using phenix.refine. Structure validation was performed with Molprobity. The processing and final refinement statistics are presented in Table 3.

Cell Lines. The breast cancer cell lines MDA-MB-468, BT474, MCF-7, SKBr3, BT20, MDA231, and T47D were chosen because they

Table 3. Crystallographic Data and Refinement Statistics

	NQO2-6A1	NQO2-5A1
space group	$P2_12_12_1$	$P2_12_12_1$
resolution (Å)	28.2–1.45 (1.51–1.45)	38.8–1.7 (1.6–1.7)
unit cell <i>a</i> , <i>b</i> , <i>c</i> (Å)	56.7, 83.5, 106.2	56.9, 84.0, 106.55
redundancy	3.7 (3.7)	3.7 (3.3)
total reflections	277 321	410 461
unique reflections	74 838	111 557
completeness (%)	99.1 (98.3)	95.0 (91.7)
R_{sym}^a (%)	5.7 (60.0)	5.1 (50.6)
$\langle I/\sigma_I \rangle$	14.9 (2.76)	16.3 (3.28)
R_{work}^b (%)	14.9	16.95
R_{free}^c (%)	16.5	20.6
Wilson B-factor (Å ²)	14.37	18.4
Ramachandran plot (%)		
favorable	95.9	96.9
allowed	3.88	2.88
generous	0	0
disallowed	0.22	0.22
rms deviations from ideal geometry		
bond length (Å)	0.012	0.007
bond angle (deg)	1.496	1.163

^a $R_{\text{sym}} = \sum h \sum i / I h_i - I h / \sum h \sum i I h_i$, where $I h$ is the mean intensity of the observations (i) of symmetry related reflections (h). ^b $R_{\text{work}} = \sum h k l^1 / \sum F_o - (h k l) - F_c(h k l)^1 / \sum h k l^1 / \sum F_o(h k l)$, where F_o and F_c are observed and calculated structure factors, respectively. ^c For the calculation of R_{free} , 5% of reflections were chosen at random to constitute a test set.

express varying levels of NQO2 (Table 2). HCT116 cells were used, as these were the cells used in previous work in our laboratory,^{12,13} thus allowing us to make toxicity comparisons with published work. The cell lines were cultured and maintained in exponential phase in RPMI-1640 medium supplemented with 10% (v/v) heat-inactivated fetal calf serum and 2 mM L-glutamine. The cells were maintained at 37 °C in a humidified incubator in an atmosphere of air plus 5% CO₂.

Assay of NQO2 Activity. Recombinant human NQO2 was diluted in 50 mM phosphate buffer to give an enzyme activity that would result in a change in optical absorbance of substrate of approximately 0.1 per minute. The enzyme reaction was started by adding 5 μL of this solution to 495 μL of 50 mM phosphate buffer at pH 7.4 containing 40 μM dichlorophenolindophenol (DCPIP) and 200 μM NRH (synthesized in house), together with various concentrations of the potential inhibitor dissolved in DMSO (final concentration 1.0% v/v). The DMSO concentration used is sufficiently small to ensure minimal perturbation of hydrogen bonding networks in aqueous NQO2 complexes. Assays were carried out in the presence or absence of 2 μM BSA. Reactions were carried out at 37 °C, and reduction of DCPIP was monitored at 600 nm in a Beckman DU 650 spectrophotometer. Concentrations resulting in 50% inhibition (IC₅₀) were determined using nonlinear curve fitting as implemented in the program Excel for which a 50% reduction of the initial rate was attained. Each measurement was made in triplicate, and the experiments were carried out three times. IC₅₀ values, given in Table 1, are derived from each of these determinations.

To measure enzyme activity in cells, exponentially growing cultures were washed with phosphate buffered saline (PBS) and scraped into 50 mM phosphate buffer (pH 7.4) containing 5 μM FAD and 250 mM sucrose. The cells were sonicated twice for 5 s on ice and centrifuged at 13 000 rpm for 15 min at 4 °C. The supernatants were collected and stored at –80 °C. Protein concentrations were determined using the

bicinchoninic acid protein assay. The assay for enzyme activity was determined by adding 10 μL of cell lysate to 490 μL of the reaction mixture described above. The difference in the rate of reaction in the presence and absence of 1 mM resveratrol was used to define the NQO2 activity in the cellular lysates.

Assays of Toxicity. Cells were seeded at 2.5×10^3 (HCT116) and between 4.0×10^3 and 10×10^3 (breast cancer cells) into 96-well plates, left overnight to attach, then exposed to the various imidazoacridin-6-ones in full growth medium for 24 or 96 h. For the shorter exposure time, drug was removed and replaced with fresh medium and cells were allowed to grow for a total of 96 h. The number of surviving cells was then determined using the MTT assay.²³ Briefly, MTT (3-(4,5-dimethylthiazol-2-yl)-2,5-diphenyltetrazolium bromide) was dissolved in sterile PBS and added to the wells at a final concentration of 1.5 mM. Cells were incubated with MTT for 4 h, medium was removed, and the remaining formazan crystals were dissolved in DMSO. Absorbance at 540 nm was then measured using a multiwell scanning spectrophotometer. Data were analyzed and curves drawn using the GraphPad Prism5 software package. Values of IC₅₀ were calculated as the concentration of compound required to reduce optical density by 50% relative to vehicle treated control cells. Since optical density is directly proportional to cell density, these values of IC₅₀ can be regarded as the concentration of compound(s) required to reduce proliferation by 50%. All toxicity experiments were repeated on at least three separate occasions. To determine the potency at which the imidazoacridin-6-ones **5a1** and **6a1** could inhibit the cellular activity of NQO2, cells were treated for 3 h with the putative inhibitors together with varying concentration of 7 plus 100 μM NRH. The cells were then washed with PBS, and fresh medium was added. The plates were incubated for a total of 96 h, and the MTT assay was used to determine cell viability.

Immunofluorescent Staining of Cells. MDA-MB-468 cells were grown on 13 mm coverslips in 6 cm Petri dishes. When cells had reached approximately 70% confluency, they were treated with varying concentrations of **5a1** or **6a1** for 3 h. Cells were then fixed on the coverslips with 3.6% formaldehyde plus 0.2% glutaraldehyde in PBS for 10 min. The coverslips were washed with 2–3 mL of PBS and the cells permeabilized with 0.1% Triton-X-100 (1 mL) for 10 min. The Triton-X-100 was removed and the cells were washed twice with PBS before being immersed in a blocking agent (10% BSA in PBS) for 30 min at room temperature. Separately, Alexa Fluor 568 phalloidin antibody (Invitrogen, A12380) was diluted in 1% BSA solution to give a dilution of 1:1000. Then 200 μL of this solution was placed on a section of Parafilm onto which coverslips were inverted. The cells were incubated for at least 20 min at room temperature, after which the coverslips were washed 3 times with PBS. The coverslips were mounted on poly-L-lysine microscope slides and stored at 4 °C in the absence of light until ready for viewing. Phalloidin was visualized at 568 nm, whereas the imidazoacridin-6-ones were excited at 340 nm with emission at 520 nm.

Measurement of Melting Temperature. DNA stability was studied by establishing the melting temperature of calf thymus DNA (20 μg/mL) in the presence of 10 μM of the imidazoacridin-6-ones in low salt phosphate buffer (7.5 mM NaH₂PO₄, 1 mM ethylenediaminetetraacetic acid, pH 7.0). Cuvettes were heated over the range 37–98 °C, and absorbance at 260 nm was read at every degree, using a Perkin-Elmer Lambda 25 UV/vis spectrophotometer. Temperature was controlled by a Perkin-Elmer Peltier temperature programmer. Relative absorbance was plotted using Origin 8.0 software, and curve fitting was done using the sigmoidal function which gave a Boltzmann distribution and regression analysis of the data. Values of T_m were read from the midpoint of the hypochromic transition curves. Values of T_m were derived from at least three independent determinations.

■ ASSOCIATED CONTENT

S Supporting Information. Figures showing microscopy results, comparisons of docked ligands, and binding affinity. This material is available free of charge via the Internet at <http://pubs.acs.org>.

Accession Codes

[†]The atomic coordinates and structure factors have been deposited in the Protein Data Bank (PDB) for NQO2 in complex with Sa1 (PDB code 3TE7) and with 6a1 (PDB code 3TEM).

■ AUTHOR INFORMATION

Corresponding Author

*Phone: +44-(0)161-275-5634. Fax: +44-(0)161-275-8342. E-mail: Karen.Nolan-2@manchester.ac.uk.

■ ACKNOWLEDGMENT

This work was funded by an MRC program grant to I.J.S. (Grant G0500366) and a project grant from the Association for International Cancer Research to K.A.N., R.A.B., R.C.W., and I.J. S. Catherine Treslove and Katherine Scott are thanked for excellent technical assistance. Dr. David Berk is thanked for advice on carrying out the fluorescent imaging.

■ ABBREVIATIONS USED

NRH, *N*-ribosylidihydronicotinamide; NQO2, NRH:quinone oxidoreductase 2; NQO1, NAD(P)H:quinone oxidoreductase 1; PDB, Protein Data Bank; NCI, National Cancer Institute; rmsd, root-mean-square deviation; QSAR, quantitative structure–activity relationship; DCPIP, dichlorophenolindophenol; PBS, phosphate buffered saline; GA, genetic algorithm; MTT, (3-(4,5-dimethylthiazol-2-yl)-2,5-diphenyltetrazolium bromide); IPTG, isopropyl β -D-1-thiogalactopyranoside; BSA, bovine serum albumin; IC₅₀, inhibitory concentration at 50%

■ REFERENCES

- (1) Phillips, R. M.; Mohammed, J.; Maitland, D. J.; Loadman, P. M.; Shnyder, S. D.; Steans, G.; Cooper, P. A.; Race, A.; Patterson, A. V.; Stratford, I. J. Pharmacological and biological evaluation of a series of substituted 1,4-naphthoquinone bioreductive drugs. *Biochem. Pharmacol.* **2004**, *68*, 2107–2116.
- (2) Gaikwad, N. W.; Yang, L.; Rogan, E. G.; Cavaliere, E. L. Evidence for NQO2-mediated reduction of the carcinogenic estrogen orthoquinones. *Free Radical Biol. Med.* **2009**, *46*, 253–262.
- (3) Dinkova-Kostova, A. T.; Talalay, P. NAD(P)H:quinone acceptor oxidoreductase 1 (NQO1), a multifunctional antioxidant enzyme and exceptionally versatile cytoprotector. *Arch. Biochem. Biophys.* **2010**, *501*, 116–123.
- (4) Iskander, K.; Paquet, M.; Brayton, C.; Jaiswal, A. K. Deficiency of NRH:quinone oxidoreductase 2 increases susceptibility to 7,12-dimethylbenz(a)anthracene and benzo(a)pyrene-induced skin carcinogenesis. *Cancer Res.* **2004**, *64*, 5925–5928.
- (5) Radjendirane, V.; Joseph, P.; Lee, Y. H.; Kimura, S.; Klein-Szanto, A. J.; Gonzalez, F. J.; Jaiswal, A. K. Disruption of the DT diaphorase (NQO1) gene in mice leads to increased menadione toxicity. *J. Biol. Chem.* **1998**, *273*, 7382–7389.
- (6) Long, D. J., 2nd; Iskander, K.; Gaikwad, A.; Arin, M.; Roop, D. R.; Knox, R.; Barrios, R.; Jaiswal, A. K. Disruption of dihydronicotinamide riboside:quinone oxidoreductase 2 (NQO2) leads to myeloid hyperplasia of bone marrow and decreased sensitivity to menadione toxicity. *J. Biol. Chem.* **2002**, *277*, 46131–46139.

- (7) Maiti, A.; Reddy, P. V.; Sturdy, M.; Marler, L.; Pegan, S. D.; Mesecar, A. D.; Pezzuto, J. M.; Cushman, M. Synthesis of casimiroin and optimization of its quinone reductase 2 and aromatase inhibitory activities. *J. Med. Chem.* **2009**, *52*, 1873–1884.

- (8) Sun, B.; Hoshino, J.; Jermihov, K.; Marler, L.; Pezzuto, J. M.; Mesecar, A. D.; Cushman, M. Design, synthesis, and biological evaluation of resveratrol analogues as aromatase and quinone reductase 2 inhibitors for chemoprevention of cancer. *Bioorg. Med. Chem.* **2010**, *18*, 5352–5366.

- (9) Conda-Sheridan, M.; Marler, L.; Park, E. J.; Kondratyuk, T. P.; Jermihov, K.; Mesecar, A. D.; Pezzuto, J. M.; Asolkar, R. N.; Fenical, W.; Cushman, M. Potential chemopreventive agents based on the structure of the lead compound 2-bromo-1-hydroxyphenazine, isolated from *Streptomyces* species, strain CNS284. *J. Med. Chem.* **2010**, *53*, 8688–8699.

- (10) Buryanovskyy, L.; Fu, Y.; Boyd, M.; Ma, Y.; Hsieh, T. C.; Wu, J. M.; Zhang, Z. Crystal structure of quinone reductase 2 in complex with resveratrol. *Biochemistry* **2004**, *43*, 1417–1426.

- (11) Nolan, K. A.; Caraher, M. C.; Humphries, M. P.; Bettley, H. A.; Bryce, R. A.; Stratford, I. J. In silico identification and biochemical evaluation of novel inhibitors of NRH:quinone oxidoreductase 2 (NQO2). *Bioorg. Med. Chem. Lett.* **2010**, *20*, 7331–7336.

- (12) Nolan, K. A.; Humphries, M. P.; Barnes, J.; Doncaster, J. R.; Caraher, M. C.; Tirelli, N.; Bryce, R. A.; Whitehead, R. C.; Stratford, I. J. Triazoloacridin-6-ones as novel inhibitors of the quinone oxidoreductases NQO1 and NQO2. *Bioorg. Med. Chem.* **2010**, *18*, 696–706.

- (13) Nolan, K. A.; Humphries, M. P.; Bryce, R. A.; Stratford, I. J. Imidazoacridin-6-ones as novel inhibitors of the quinone oxidoreductase NQO2. *Bioorg. Med. Chem. Lett.* **2010**, *20*, 2832–2836.

- (14) Ferry, G.; Hecht, S.; Berger, S.; Moulharat, N.; Coge, F.; Guillaumet, G.; Leclerc, V.; Yous, S.; Delagrangue, P.; Boutin, J. A. Old and new inhibitors of quinone reductase 2. *Chem.-Biol. Interact.* **2010**, *186*, 103–109.

- (15) Mailliet, F.; Ferry, G.; Vella, F.; Berger, S.; Cogé, F.; Chomarot, P.; Mallet, C.; Guénin, S. P.; Guillaumet, G.; Viaud-Massuard, M. C.; Yous, S.; Delagrangue, P.; Boutin, J. A. Characterization of the melatoninergic MT3 binding site on the NRH:quinone oxidoreductase 2 enzyme. *Biochem. Pharmacol.* **2005**, *71*, 74–88.

- (16) Rix, U.; Hantschel, O.; Dürmberger, G.; Rensing, R.; Rix, L. L.; Panyavsky, M.; Fernbach, N. V.; Kaupe, I.; Bennett, K. L.; Valent, P.; Colinge, J.; Köcher, T.; Superti-Furga, G. Chemical proteomic profiles of the BCR-ABL inhibitors imatinib, nilotinib, and dasatinib reveal novel kinase and nonkinase targets. *Blood* **2007**, *110*, 4055–4063.

- (17) Serin, M.; Gülbaş, H.; Gürses, I.; Erkal, H. S.; Yücel, N. The histopathological evaluation of the effectiveness of melatonin as a protectant against acute lung injury induced by radiation therapy in a rat model. *Int. J. Radiat. Biol.* **2007**, *83*, 187–193.

- (18) Li, M.; Abdollahi, A.; Gröne, H. J.; Lipson, K. E.; Belka, C.; Huber, P. E. Late treatment with imatinib mesylate ameliorates radiation-induced lung fibrosis in a mouse model. *Radiat. Oncol.* **2009**, *21*, 4:66.

- (19) Cholody, W. M.; Martelli, S.; Konopa, J. 8-Substituted 5-[(aminoalkyl)amino]-6H-*v*-triazolo[4,5,1-*de*]acridin-6-ones as potential antineoplastic agents. Synthesis and biological activity. *J. Med. Chem.* **1990**, *33*, 2852–2856.

- (20) Knox, R. J.; Jenkins, T. C.; Hobbs, S. M.; Chen, S.; Melton, R. G.; Burke, P. J. Bioactivation of 5-(aziridin-1-yl)-2,4-dinitrobenzamide (CB 1954) by human NAD(P)H quinone oxidoreductase 2: a novel co-substrate-mediated antitumor prodrug therapy. *Cancer Res.* **2000**, *60*, 4179–4186.

- (21) Foster, C. E.; Bianchet, M. A.; Talalay, P.; Zhao, Q.; Amzel, L. M. Crystal structure of human quinone reductase type 2, a metalloflavoprotein. *Biochemistry* **1999**, *38*, 9881–9886.

- (22) Winger, J. A.; Hantschel, O.; Superti-Furga, G.; Kuriyan, J. The structure of the leukemia drug imatinib bound to human quinone reductase 2 (NQO2). *BMC Struct. Biol.* **2009**, *9*, 7.

- (23) Nolan, K. A.; Doncaster, J. R.; Dunstan, M.; Scott, K. A.; Frenkel, A. D.; Siegel, D.; Ross, D.; Barnes, J.; Levy, C.; Whitehead, R. C.; Stratford, I. J.; Bryce, R. A. Synthesis and biological evaluation of

coumarin-based inhibitors of NAD(P)H: quinone oxidoreductase-1 (NQO1). *J. Med. Chem.* **2009**, *52*, 7142–7156.

(24) Kabsch, W. Evaluation of single-crystal X-ray diffraction data from a position-sensitive detector. *J. Appl. Crystallogr.* **1988**, *21*, 916–924.

(25) Adams, P. D.; Afonine, P. V.; Bunkóczi, G.; Chen, V. B.; Davis, I. W.; Echols, N.; Headd, J. J.; Hung, L. W.; Kapral, G. J.; Grosse-Kunstleve, R. W.; McCoy, A. J.; Moriarty, N. W.; Oeffner, R.; Read, R. J.; Richardson, D. C.; Richardson, J. S.; Terwilliger, T. C.; Zwart, P. H. PHENIX: a comprehensive Python-based system for macromolecular structure solution. *Acta Crystallogr., Sect. D: Biol. Crystallogr.* **2010**, *66*, 213–221.

(26) Emsley, P.; Cowtan, K. Coot: model-building tools for molecular graphics. *Acta Crystallographica D Biol Crystallogr.* **2004**, *60*, 2126–2132.